SYNCHRONIZATION OF CHAOTIC SYSTEMS BY USING OCCASIONAL COUPLING

A THESIS

SUBMITTED TO THE DEPARTMENT OF ELECTRICAL AND

ELECTRONICS ENGINEERING

AND THE INSTITUTE OF ENGINEERING AND SCIENCES

OF BILKENT UNIVERSITY

IN PARTIAL FULFILLMENT OF THE REQUIREMENTS

FOR THE DEGREE OF

MASTER OF SCIENCE

By

Moez Feki

June 1997

SYNCHRONIZATION OF CHAOTIC SYSTEMS BY USING OCCASIONAL COUPLING

A THESIS

SUBMITTED TO THE DEPARTMENT OF ELECTRICAL AND

ELECTRONICS ENGINEERING

AND THE INSTITUTE OF ENGINEERING AND SCIENCES

OF BILKENT UNIVERSITY

IN PARTIAL FULFILLMENT OF THE REQUIREMENTS

FOR THE DEGREE OF

MASTER OF SCIENCE

By

Moez Feki

June 1997

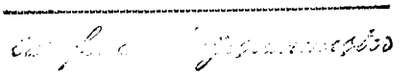

I certify that I have read this thesis and that in my opinion it is fully adequate, in scope and in quality, as a thesis for the degree of Master of Science.

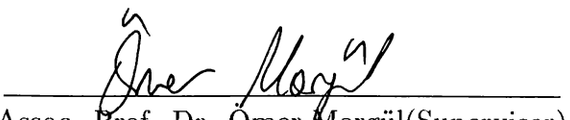

Assoc. Prof. Dr. Ömer Morgül(Supervisor)

I certify that I have read this thesis and that in my opinion it is fully adequate, in scope and in quality, as a thesis for the degree of Master of Science.

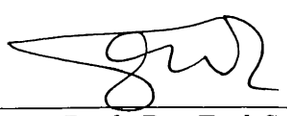

Prof. Dr. Erol Sezer

I certify that I have read this thesis and that in my opinion it is fully adequate, in scope and in quality, as a thesis for the degree of Master of Science.

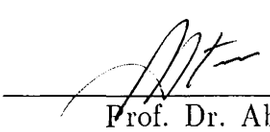

Prof. Dr. Abdullah Atalar

Approved for the Institute of Engineering and Sciences:

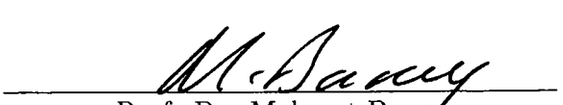

Prof. Dr. Mehmet Baray
Director of Institute of Engineering and Sciences

ABSTRACT

SYNCHRONIZATION OF CHAOTIC SYSTEMS BY USING OCCASIONAL COUPLING

Moez Feki
M.S. in Electrical and Electronics Engineering
Supervisor: Assoc. Prof. Dr. Ömer Morgül
June 1997

Nonlinear and chaotic systems are difficult to control due to their unstable and unpredictable nature. Although, much work has been done in this area, synchronization of chaotic systems still remains a worthwhile endeavor.

In this thesis, a method to synchronize systems, inherently operating in a chaotic mode, by using occasional coupling is presented. We assume that a master-slave synchronizing scheme is available. This approach consists of coupling and uncoupling the drive and response systems during some alternated intervals. It is then shown how this synchronization method can be used to transmit information on a chaotic carrier. The applicability of this method will be illustrated using Lorenz system as the chaotic oscillator.

Keywords : Chaotic systems, Lorenz system, Chaos synchronization.

ÖZET

ARASIRA BAĞLANTI YOLUYLA KAOTİK SİSTEMLERİN EŞZAMANLAMASI

Moez Feki
Elektrik ve Elektronik Mühendisliği Bölümü Yüksek Lisans
Tez Yöneticisi: Doç. Dr. Ömer Morgül
Haziran 1997

Doğrusal olmayan ve kaotik sistemler, çözümlerinin kestirilmesi ve kararsız yapıları dolayısıyla kontrol edilmeleri oldukça güç olan sistemlerdir. Bu konuda son yıllarda oldukça çalışma yapılmış olmasına rağmen kaotik sistemlerin eşzamanlaması hala araştırmaya değer bir konu olarak görülmektedir.

Bu çalışmada kaotik modda çalışan sistemleri arasıra bağlantı yoluyla eşzamanlaması metodu incelenmiştir. Bu çalışmada bir sürücü ve bir alıcı sistemi eşzamanlayacak bir yönetim önceden var olduğunu kabul edeceğiz. Önerilen arasıra bağlantı yönteminde sürücü ve alıcı sistemler ard arda gelen belli zaman aralıklarında bağlanacak ve bağlantı kesilecektir. Daha sonra bu yöntemin sürücü ile alıcı arasında nasıl bilgi aktarımında kullanılacağı incelenecektir. Bu yöntemin uygulanabilirliği Lorenz sistemi kullanılarak gösterilecektir.

Anahtar Kelimeler : Kaotik sistemler, Lorenz sistemler, Kaos eşzamanlaması.

ACKNOWLEDGEMENT

I would like to express my deep gratitude to my supervisor Assoc. Prof. Dr. Ömer Morgül for his guidance, suggestions and valuable encouragement throughout the development of this thesis.

I would like to thank Prof. Dr. Abdullah Atalar and Prof. Dr. Erol Sezer for reading and commenting on the thesis and for the honor they gave me by presiding the jury.

I am forever indebted to my family for their patience and support.

I thank my friends for everything.

Sincere thanks are also extended to everybody who has helped in the development of this thesis.

To my family.
and
To Olfa, who has added
little joyful chaos to my life.

Contents

List of Figures

Chapter 1

Introduction: A New Age of Dynamics

"Until recently, chaotic behavior
was a nuisance in engineering..."
L.O. Chua and M. Hasler

1.1 What is chaotic dynamics?

Throughout the history of science, complex nonlinear phenomena have been noticed by experimentalists but more often than not, have been disregarded because the concepts for explaining them simply did not exist.

For some, the study of dynamics began and ended with Newton's law of **F=ma**. We were told that if the forces between particles and their initial positions and velocities were given, one could predict the motion or history of a system forever into the future, given a big enough computer. However, the arrival of large and fast computers has not fulfilled the promise of infinite predictability in dynamics. In fact, it has been discovered quite recently that the motion of very simple dynamical systems cannot always be predicted far into the future. Such dynamical systems, which in the papers are dubbed chaotic systems, (or said to

exhibit chaos: the origin of the word chaos is a Greek verb which means to gape open and which was often used to refer to the primeral emptiness of the universe before things came into being.) Such systems are defined to be **aperiodic, bounded** dynamics in a **deterministic** systems with **sensitive dependence on initial conditions,** see [1].

Each of these terms has a specific meaning, see [1]:

- **Aperiodic**: means that the same state is never repeated twice. However, in practice, by either graphically iterating or using a computer with finite precision, we eventually may return to the same value. Although, a computer simulation or graphical iteration always leaves some doubt about whether the behavior is periodic, the presence of very long cycles or of aperiodic dynamics in computer simulations is partial evidence for chaos.
- **Bounded**: means that on successive iterations the state stays in finite range and does not approach $\pm\infty$.
- **Deterministic**: means that there is a definite rule with no random terms governing the dynamics (e.g, Lorenz's equations, Rossler's equations ...). In principle, for a deterministic system x_0 can be used to calculate all future values of $x(t)$.
- **Sensitive dependence on initial conditions.**: means that two points that are initially close will drift apart as time proceeds. This is an essential aspect of chaos. It means that we may be able to predict what happens for short times, but that over long times prediction will be impossible since we can never be certain of the exact value of the initial condition in any realistic system.

Loss of information about initial conditions is, indeed, a property of chaotic system. Suppose one has the ability to measure a position with accuracy Δx and a velocity with accuracy Δv, then in the position-velocity plane (known as the phase plane) we can divide up the space into areas of size $\Delta x \Delta v$ as shown in Figure 1.1.

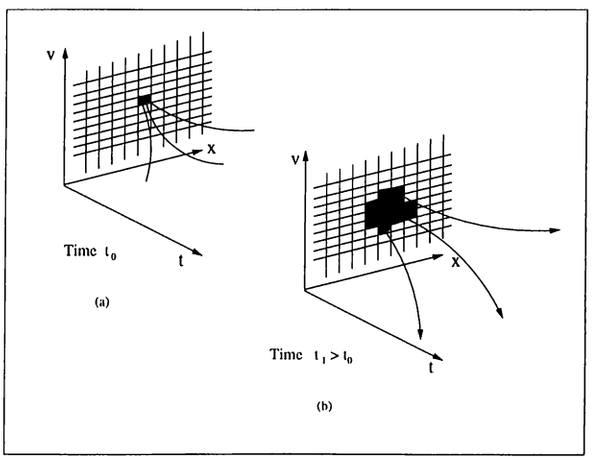

Figure 1.1: Uncertainty growth in chaotic dynamics.

If we are given initial conditions to the delineated accuracy, we know the system is somewhere in the shaded box in the phase plane. But if the system is chaotic, this uncertainty grows in time to $N(t)$ boxes as shown in Figure 1.1-b. The growth in uncertainty given by $N = N_0 e^{ht}$ is another property of chaotic systems. The constant h is related to Lyapunov exponent, see [2]. Lyapunov exponents quantify the average exponential rates of separation of trajectories along the flow. For instance, the flow in a neighborhood of asymptotically stable trajectory is contracting so the Lyapunov exponents are negative, whereas, sensitive dependence on initial conditions results from positive Lyapunov exponents. In fact, since chaotic dynamics are bounded, the divergence of chaotic orbits can be only locally exponential.

One more characteristics of chaotic vibrations, is the broadness of the spectrum of Fourier transform, when motion is generated by single frequency that is if we consider, for example, the differential equation

$$\ddot{x} + \frac{1}{4}\dot{x} - x + x^3 \;=\; 0.3cos\omega t \;,\; \omega = 1.$$

we obtain a wide spectrum of the output signal $x(t)$ as shown in Figure 1.2.

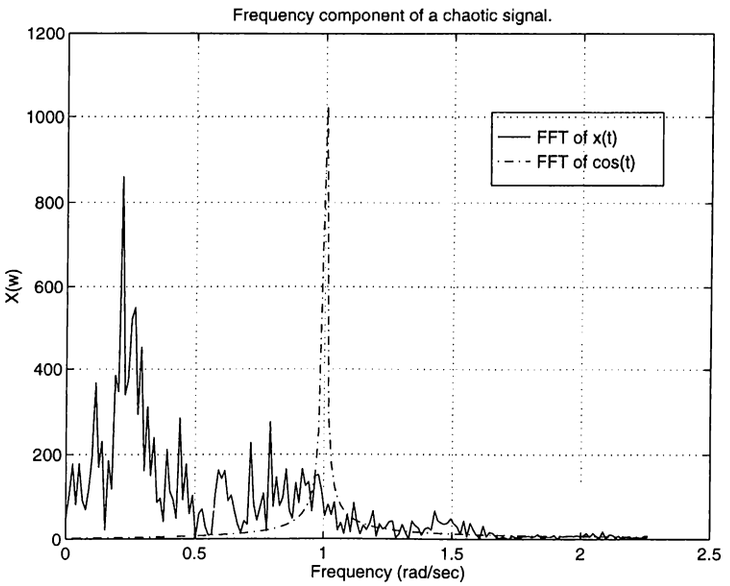

Figure 1.2: Broadness of the spectrum of a chaotic signal.

1.2 Where have chaotic vibrations been observed?

Chaotic oscillations are the emergence of random like motions from completely deterministic systems. Such motions had been known in fluid mechanics, but they have recently been observed in low-order mechanical and electrical systems and even in simple one-degree-of-freedom problems, see [3].

In 1963, an atmospheric scientist named E.N.Lorenz of M.I.T proposed a simple model for thermally induced fluid convection in the atmosphere. Fluid heated from below becomes lighter and rises while heavier fluid falls under gravity. Such motions often produce convection rolls similar to the motion of fluid in a circular torus as shown in Figure 1.3.

In Lorenz's mathematical model of convection, three state variables are used (x, y, z). The variable x is proportional to the amplitude of the fluid velocity circulation in the fluid ring, while y and z measure the distribution of temperature around the ring. The so-called Lorenz equations may be derived formally from

the Navier-Stokes partial differential equations of fluid mechanics. The non-dimensional forms of Lorenz's equations are:

$$\begin{aligned} \dot{x} &= \sigma(y - x) \ , \\ \dot{y} &= -xz + rx - y \ , \\ \dot{z} &= xy - bz \ . \end{aligned} \tag{1.1}$$

where σ, r and b are some positive real constants.

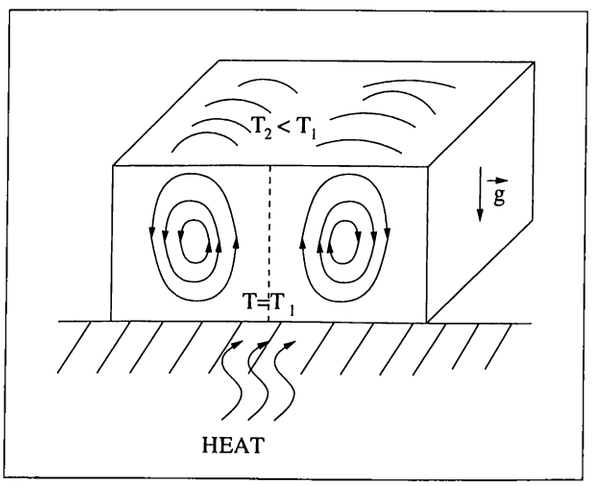

Figure 1.3: Motion of heated fluid.

It was Lorenz's insistence in the years following 1963 that chaotic motions produced by the system defined in (1.1) were not artifacts of computer simulation but were inherent in the equations themselves, that led mathematicians to study these equations further. Since 1963, hundreds of papers have been written about these equations and this example has become a classic model for chaotic dynamics.

Chaotic phenomena were also observed in mechanical systems, herein, we cite two simple examples, [3], [4]. The first is a thought experiment of an idealized billiard ball which bounces off the sides of an elliptical billiard table. When damping is neglected (ideally smooth table) and elastic impact is assumed, the energy remains conserved (boundedness of the motion) but the ball may wonder about the table without exactly repeating a previous motion of certain elliptically

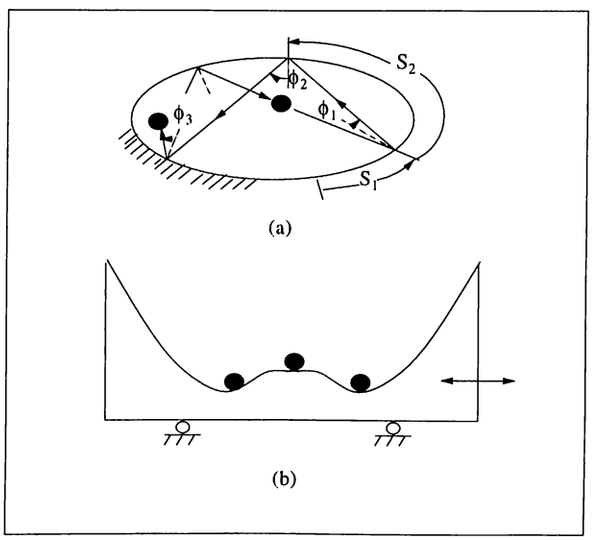

Figure 1.4: (a) The motion of a ball after several impacts with an elliptically shaped billiard table. The motion can be described by a set of discrete numbers (s_i, Φ_i) called a map. (b) The motion of a particle in a two-well potential under excitation.

shaped tables. Another example, depicted in Figure 1.4-b, is the ball in a two-well potential. Here the ball has two equilibrium states when the table or base does not vibrate. However, when the table vibrates with periodic translating motion of large enough amplitude, the ball will jump from one well to the other in an apparently random manner, that is an input of one frequency leads to a broad spectrum output (broadness of the spectrum).

Chaotic vibrations can also be observed in electric systems. This type of chaotic dynamical systems illustrate a revolution in the field of chaos. In fact researchers preferred the electrical systems for its being simple and clear enough to be analyzed. Indeed, in the rush to explain chaotic dynamics in physical systems, there is a temptation to propose mathematical models that emulate the classic chaos paradigms. This could be easily done in the case of electrical circuits, rather than in mathematical or fluid systems. Moreover, the chaotic vibration or sounds can be clearly observed on oscilloscope or heard in such cases.

A simple circuit which was known to exhibit chaos, is depicted in Figure 1.5 it was called the Chua circuit (named after Leon O. Chua).

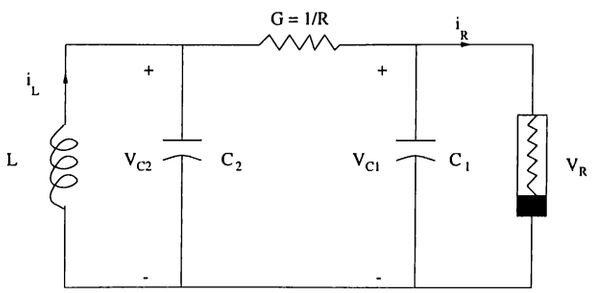

Figure 1.5: Chua's circuit.

A somewhat peculiar aspect in the literature is the choice of Chua's circuit by many authors both as a vehicle of discourse and as a chaotic circuit building block for applications. In fact, many other circuits and systems have also been known to exhibit chaotic behavior. However, Chua's circuit appears to be the chaotic circuit of choice because it is the simplest chaotic circuit, it has been widely studied, it is easily realizable in the laboratory, and it is capable of exhibiting virtually all reported generic bifurcation and chaotic phenomena of third order autonomous systems. Therefore, it serves as a workhorse for testing concepts, comparing results, and designing engineering application.

In the next chapter, we would focus on chaotic phenomena created in three dimensional systems, by giving concrete simulation as well as numerical results, together with theoretical justifications. In the third chapter we would introduce different methods to synchronize chaotic systems. Next, our new approach to synchronize chaotic systems will be discussed, and then its use for message transmission will be presented. The fifth chapter is devoted to present the experimental work and results. Eventually we shall conclude this work by stating some remarks.

Chapter 2

Three-Dimensional Chaotic Systems

The world is an ∞-dimensional chaotic system.

2.1 Lorenz System

2.1.1 Mathematical Model

In order to approximate the motion of thermally induced fluid convection in the atmosphere, E. N. Lorenz had proposed the following non dimensional system of differential equations (the Lorenz model).

$$\begin{aligned} \dot{x} &= \sigma(y - x) \ , \\ \dot{y} &= rx - y - xz \ , \\ \dot{z} &= xy - bz \ . \end{aligned} \tag{2.1}$$

where the dot refers to the differentiation with respect to time and σ, r, and b are real positive parameters. Note that the only nonlinear terms are xz and xy in the second and third equations.

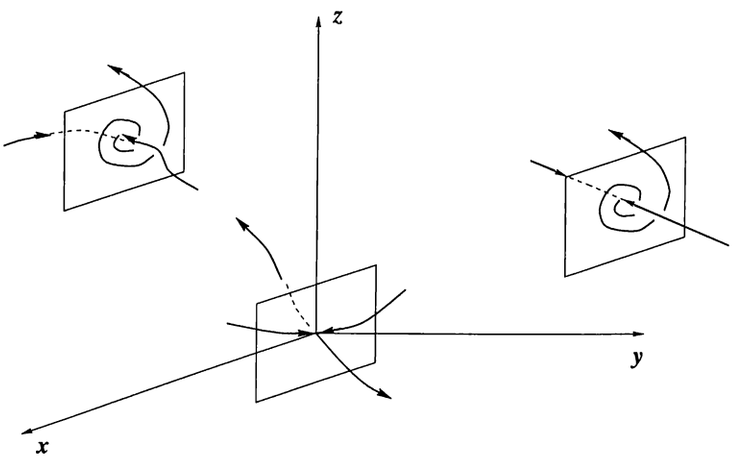

Figure 2.1: Sketch of local motion near the three equilibria for the Lorenz system.

The importance of this model in not that it quantitatively describes the hydrodynamic motion, but rather that it illustrates how a simple model can produce very rich and varied forms of dynamics, depending on the values of the parameters in the equations.

For the parameter values $(\sigma, r, b) = (10, 28, 8/3)$ (studied by Lorenz) or $(10, 20, 1)$ that will be studied in chapter four, there are three equilibrium points, all of them unstable. The origin is a saddle point, while the other two are unstable foci or spiral equilibrium points (Figure 2.1). Nevertheless, globally one can show that the motion is bounded. That is the trajectories do not diverge nor converge to a specified limit but remain confined to an ellipsoidal region of phase space. Indeed, this was a property established by Lorenz, see [2].

property 2.1 *All solutions of the Lorenz system remain bounded in phase space for all times.*

Proof: let $u = z - r - \sigma$, then (2.1) becomes:

$$\begin{aligned} \dot{x} &= \sigma(y - x) \ , \\ \dot{y} &= -x(u + \sigma) - y \ , \\ \dot{z} &= xy - b(u + r + \sigma) \ . \end{aligned}$$

Now let's consider the positive definite Lyapunov function

$$V(x,y,u) = \frac{1}{2}x^2 + \frac{1}{2}y^2 + \frac{1}{2}u^2 \quad .$$

Then we have

$$\begin{aligned} \dot{V}(x,y,u) &= x\sigma(y-x) - y(y+x(u+\sigma)) + u(-b(u+r+\sigma)+xy) \\ &= \sigma xy - \sigma x^2 - y^2 - xy\sigma - xyu - bu^2 - bru - b\sigma u + uxy \\ &= -\sigma x^2 - y^2 - b(u^2 + ru + \sigma u). \end{aligned} \tag{2.2}$$

Since all constants are positive, it easily follows that for $u > 0$ or $u < -(\sigma + r)$ (or equivalently for $z > \sigma + r$ or $z < 0$, respectively), $\dot{V} < 0$ hence the Lyapunov function decreases outside a bounded region (e.g. in the region $x^2 + y^2 + u^2 > 2(\sigma + r)$). This proves that the solutions remain bounded. In the sequel, we will use this property to prove some other important facts.

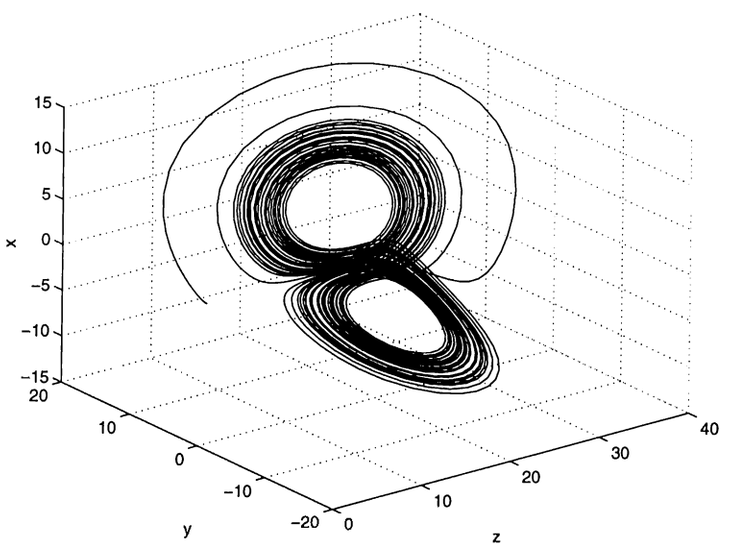

Figure 2.2: Dynamics of Lorenz system.$(\sigma, r, b) = (10, 20, 1)$ (MATLAB simulation)

2.1.2 Electronic Implementation

An electronic circuit implementation of the Lorenz system has been suggested in [5]. In fact, the implementation was not direct, because the state variables of the Lorenz system occupy a wide dynamic range with values that exceed reasonable power supply limits. A simple remedy to this difficulty, is scaling the state variable as follows: $x \rightarrow x/10$, $y \rightarrow y/10$, $z \rightarrow z/20$. With these new state variables the Lorenz system equations are transformed to:

$$\begin{aligned} \dot{x} &= \sigma(y - x) \ , \\ \dot{y} &= rx - y - 20xz \ , \\ \dot{z} &= 5xy - bz \ . \end{aligned} \tag{2.3}$$

An analog circuit implementation of (2.3) is shown in Figure 2.3. The operational amplifiers and the associated circuitry perform the operations of addition, subtraction, and integration. The multipliers implement the non-linearities in the second and third equations. By applying circuit theory techniques to analyze the circuit, the following state equations that governs the dynamical behavior of the circuit can be obtained.

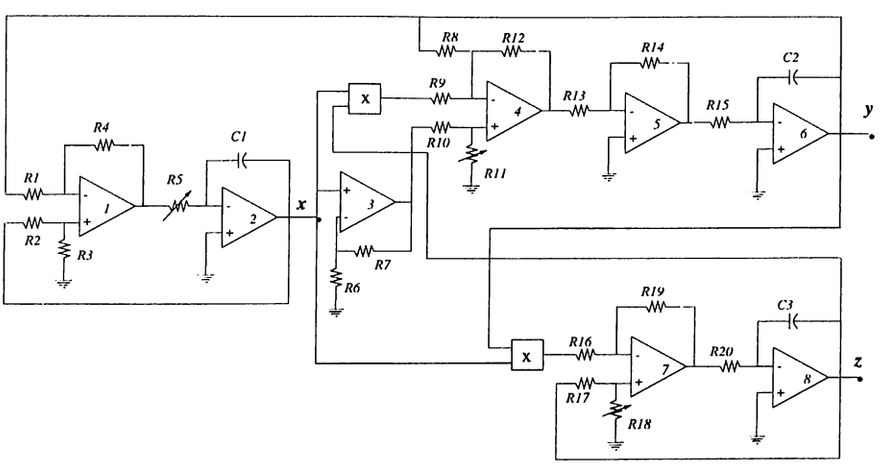

Figure 2.3: Lorenz-based chaotic circuit.

$$\dot{x} = \frac{1}{R_5 C_1}\left[\frac{R_4}{R_1}y - \frac{R_3}{R_2 + R_3}(1 + \frac{R_4}{R_1})x\right] \ ,$$

$$\dot{y} = \frac{1}{R_{15}C_2}\left[\frac{R_{11}}{R_{10}+R_{11}}(1+\frac{R_{12}}{R_8}+\frac{R_{12}}{R_9})(1+\frac{R_7}{R_6})x - \frac{R_{12}}{R_8}y - \frac{R_{12}}{R_9}xz\right], \quad (2.4)$$

$$\dot{z} = \frac{1}{R_{20}C_3}\left[\frac{R_{19}}{R_{16}}xy - \frac{R_{18}}{R_{17}+R_{18}}(1+\frac{R_{19}}{R_{16}})z\right]$$

where x, y and z are the voltages measured at the outputs of op-amps 2, 6 and 8, respectively.

We note that the circuit is large compared to Chua's circuit. Moreover, it contains integraters which are not convenient in electronic circuits design.

The component values [1] of the circuit can be appropriately chosen to meet different parameter combinations by changing R_5, R_{11}, and R_{18}, and the circuit time scale can be easily adjusted by changing the values of the capacitors. Figure 2.4 depicts the behavior of the circuit projected onto the xy-plane and xz-plane, respectively. These data were obtained from H-spice simulation. Note that the multipliers were modeled by H-spice nonlinear voltage controlled voltage source, due to nonexistence of AD632AD macro-model.

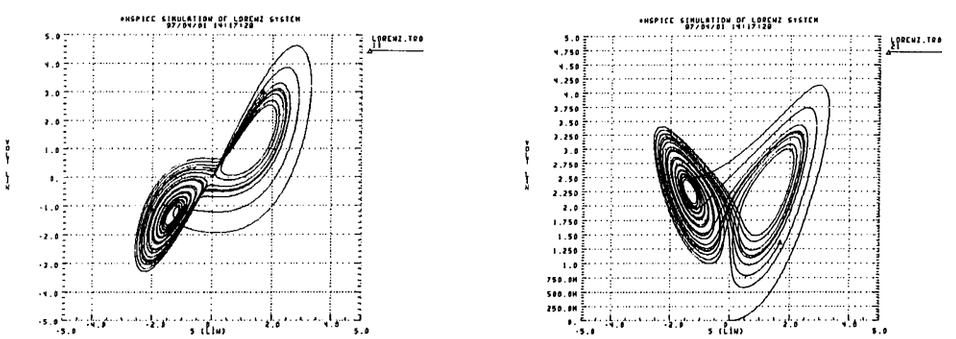

Figure 2.4: H-spice simulation of the Lorenz-based chaotic circuit. The first and second graphs represent: x-signal vs y-signal and x-signal vs z-signal respectively.

[1] Resistors($k\Omega$): R1, R2, R3, R4, R6, R7, R13, R14, R16, R17, R19=100 R5, R10=49.9 R8=200 R9, R12=10 R11=63.4 R15=40.2 R18=66.5 R20=158. Capacitors(pF): C1, C2, C3=500. Op-Amps (1) ...(8): LF353 Multipliers: AD632AD.

2.2 Chua's Circuit

2.2.1 Circuit Dynamics

The Chua's circuit shown in Figure 2.5-a consists of two capacitors (C_1 and C_2), inductor (L), a linear resistor (G) and only one nonlinear resistor, the characteristic of which, is described by Figure 2.5-b. This characteristic is defined analytically as follows:

$$i_R = f(v_R) = \begin{cases} G_b v_R + (G_b - G_a)E & if \quad v_R < -E \\ G_a v_R & if \quad -E \leq v_R \leq E \\ G_b v_R + (G_a - G_b)E & if \quad v_R > E \end{cases} \tag{2.5}$$

where $E > 0$ and $G_a < G_b < 0$. There are simple and yet very important reasons for choosing a piecewise-linear resistor instead of other nonlinear resistors. First of all, it is easy to implement. If $f(.)$ is, for example, a third order polynomial, then it will be extremely difficult to implement. The piecewise-linearity also simplifies rigorous analysis in a drastic manner. Namely, the state space can be decomposed into three regions in each of which the dynamics is linear so that trajectory can be expressed as a composition of linear flow.

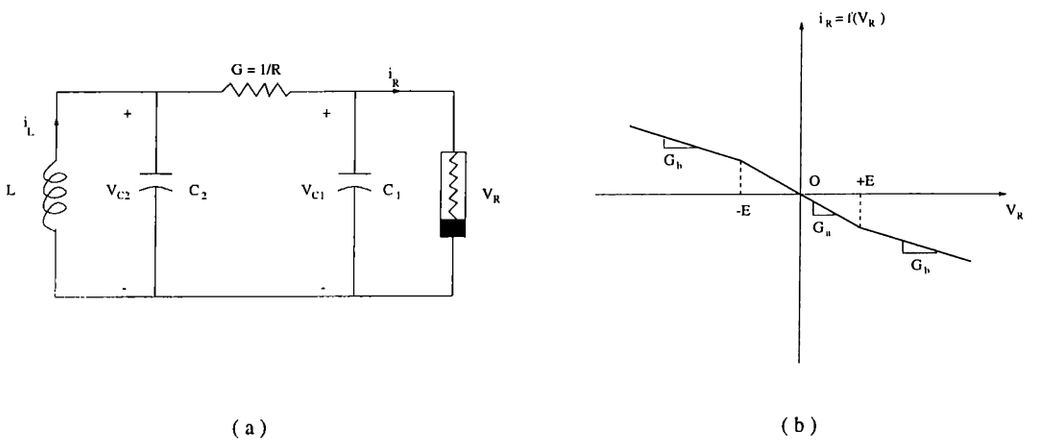

Figure 2.5: Chaotic system.(a)Chua's circuit.(b)Nonlinear resistor characteristic.

One can write down, then, explicit bifurcation equations. Using Kirchoff's voltage and current laws, this circuit may be described by three ordinary differential equations. By choosing v_{C1}, v_{C2} and i_L as state variables, we obtain the following equations:

$$\frac{dv_{C1}}{dt} = \frac{G}{C_1}(v_{C2} - v_{C1}) - \frac{1}{C_1}f(v_{C1}) \ , \tag{2.6}$$

$$\frac{dv_{C2}}{dt} = \frac{G}{C_2}(v_{C1} - v_{C2}) + \frac{1}{C_2}i_L \ , \tag{2.7}$$

$$\frac{di_L}{dt} = -\frac{1}{L}v_{C2} \ . \tag{2.8}$$

The rich dynamical behavior of Chua's circuit was confirmed by computer simulations and experiments, see [6][7]. It has been shown that different values of circuit elements lead to different dynamics. With an appropriate choice of element values, the circuit can be made to behave in the chaotic domain. To investigate the circuit, let us substitute (2.5) in (2.6). Then we may decompose the system of equations into three distinct affine regions: $v_{C1} < -E$, $|v_{C1}| \leq E$, and $v_{C1} > E$. We denote these regions by $D_{-1}, D_0, \text{and} D_1$, respectively. Using piecewise-linear analysis, we examine each region separately, and then superpose all regions together. We look at D_0 first.

The Middle Region ($|v_{C1}| \leq E$)

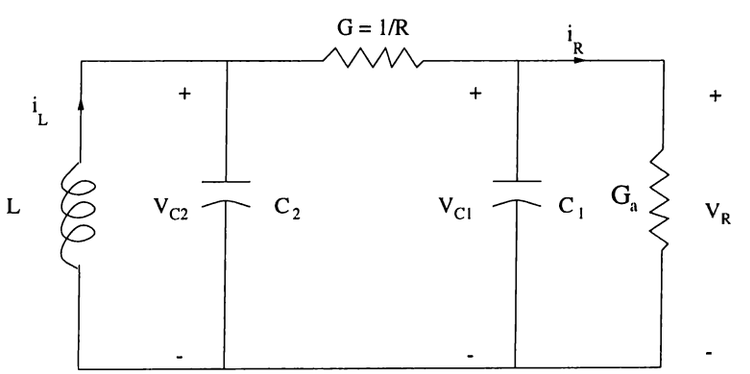

Figure 2.6: Equivalent of Chua's circuit in the D_0 region.

When $|v_{C1}| \leq E$, the Chua's circuit is described by the following system.

$$\begin{aligned} \frac{dv_{C1}}{dt} &= \frac{G}{C_1}v_{C2} - \frac{G+G_a}{C_1}v_{C1} \quad , \\ \frac{dv_{C2}}{dt} &= \frac{G}{C_2}(v_{C1} - v_{C2}) + \frac{1}{C_2}i_L \quad , \\ \frac{di_L}{dt} &= -\frac{1}{L}v_{C2} \quad . \end{aligned}$$

The D_0 equivalent circuit is simply the linear parallel RLC circuit shown in Figure 2.6. This linear circuit has a single equilibrium point at the origin whose stability is specified by the eigenvalues of the Jacobian matrix of the system:

$$J_{D_0} = \begin{bmatrix} -\frac{G+G_a}{C_1} & \frac{G}{C_1} & 0 \\ \frac{G}{C_2} & -\frac{G}{C_2} & \frac{1}{C_2} \\ 0 & -\frac{1}{i_L} & 0 \end{bmatrix}.$$

By using the element values ($L = 18mH, C_1 = 10nF, C_2 = 100nF, R = 1830\Omega$ $G_a = -757\mu s$ *and* $G_b = -411\mu s$), we obtain the following eigenvalues of J_{D_0}:

$$\begin{aligned} \gamma_0 &\approx 41233 \\ \sigma_0 \pm j\omega_0 &\approx -5339 \pm j21402 \end{aligned}$$

Associated with the unstable real eigenvalue γ_0 is an eigenvector $E^r(0)$, whereas the complex eigenvector associated with $\sigma_0 \pm j\omega_0$ span a complex eigenplane denoted by $E^c(0)$.

Qualitative Description of the D_0 Dynamics: "A trajectory starting from some initial state in the D_0 region may be decomposed into its components along the complex eigenplane $E^c(0)$ and along the eigenvector $E^r(0)$. When $\gamma_0 > 0$ and $\sigma_0 < 0$, the component along $E^c(0)$ spirals toward the origin along this plane while the component in the direction $E^r(0)$ grows exponentially. Adding the two components, we see that a trajectory starting slightly above the stable complex eigenplane $E^c(0)$ spirals toward the origin along the $E^c(0)$ direction all the while being pushed away from $E^c(0)$ along the unstable direction $E^r(0)$. As the (stable) component along $E^c(0)$ shrinks in magnitude, the unstable component grows

exponentially, and the trajectory follows a helix of exponentially decreasing radius whose axis lies in the direction of $E^r(0)$", see [6].

Now let's analyze D_{-1} and D_{+1}

The Outer Region ($|v_{C1}| > E$)

In the outer regions, Chua's circuit is described by

$$\begin{aligned} \frac{dv_{C1}}{dt} &= \frac{G}{C_1}v_{C2} - \frac{G+G_b}{C_1}v_{C1} - i_{NL} \ , \\ \frac{dv_{C2}}{dt} &= \frac{G}{C_2}(v_{C1} - v_{C2}) + \frac{1}{C_2}i_L \ , \\ \frac{di_L}{dt} &= -\frac{1}{L}v_{C2} \ . \end{aligned}$$

where $i_{NL} = (G_b - G_a)E$ when $v_{C1} < E$ (the D_{-1} region) and $i_{NL} = (G_a - G_b)E$ when $v_{C1} > E$ (the D_{+1} region). The equivalent circuit consists of a linear parallel RLC circuit with shunt DC current source i_{NL} as shown in Figure 2.7. The equilibrium points P_- and P_+ of the outer regions are obtained from the DC solution of the equivalent circuit shown in Figure 2.7 by short-circuiting the inductor and open-circuiting the capacitors. Therefore the equilibrium points are:

$$P_- = \begin{bmatrix} \frac{G_a-G_b}{G+G_b}E \\ 0 \\ \frac{G(G_b-G_a)}{G+G_b}E \end{bmatrix}, \qquad P_+ = \begin{bmatrix} \frac{G_b-G_a}{G+G_b}E \\ 0 \\ \frac{G(G_a-G_b)}{G+G_b}E \end{bmatrix}$$

It is worth noting that these equilibrium points are situated inside their corresponding regions, hence, this circuit has three equilibrium points. The stability of the equilibrium points is determined by the eigenvalues of the Jacobian matrix

$$J_{D_{-1},D_{+1}} = \begin{bmatrix} -\frac{G+G_b}{C_1} & \frac{G}{C_1} & 0 \\ \frac{G}{C_2} & -\frac{G}{C_2} & \frac{1}{C_2} \\ 0 & -\frac{1}{i_L} & 0 \end{bmatrix}.$$

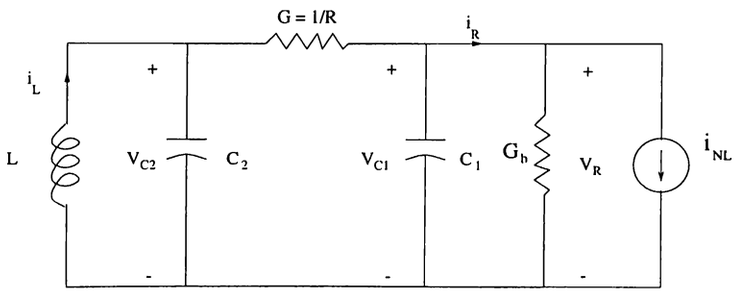

Figure 2.7: Equivalent of Chua's circuit in the $D_{\pm 1}$ regions.

Notice that both D_{-1} and D_{+1} regions have the same Jacobian matrix, hence the corresponding dynamical behaviors are similar. The eigenvalues, for the corresponding element values are

$$\begin{aligned} \gamma_1 &\approx -22050 \\ \sigma_1 \pm j\omega_1 &\approx 924 \pm j19188 \end{aligned}$$

Qualitative Description of the Dynamics for $|v_{C1}| > E$: "Associated with the stable real eigenvalue γ_1 in the D_1 region is the eigenvector $E^r(P_+)$. The real and imaginary parts of the complex eigenvectors associated with $\sigma_1 \pm j\omega_1$ define a complex eigenplane $E^c(P_+)$.

A trajectory starting from some initial state in the D_1 region may be decomposed into its components along the complex eigenplane $E^c(P_+)$ and the eigenvector $E^r(P_+)$. When $\gamma_1 < 0$ and $\sigma_1 > 0$, the component on $E^c(P_+)$ spirals away from P_+ along this plane while the component in the direction of $E^r(P_+)$ tends asymptotically toward P_+. Adding the two components, we see that a trajectory starting close to that stable real eigenvector $E^r(P_+)$ above the complex eigenplane moves toward $E^c(P_+)$ along a helix of exponentially increasing radius. Since the component along $E^r(P_+)$ shrinks exponentially in magnitude and the component on $E^c(P_+)$ grows exponentially, the trajectory is quickly flattened onto $E^c(P_+)$, where it spirals away from P_+ along the complex eigenplane. By symmetry, the equilibrium P_- has three eigenvalues: γ_1 and $\sigma_1 \pm j\omega_1$, therefore similar dynamics as for P_+" , see [6].

The double scroll depicted in Figure 2.8 delineates the stretching and folding

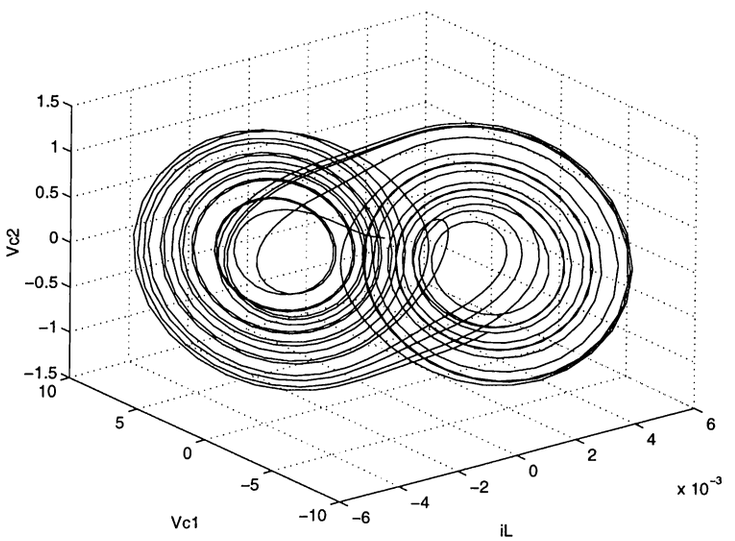

Figure 2.8: MATLAB simulation of the Chua's circuit describing system.

of the vector field. These were the results of numerical (MATLAB) simulation of the system of differential equations (2.6), (2.7), and (2.8) with the element values previously indicated.

2.2.2 Electronic Implementation

The Chua's circuit has been implemented in many different ways using standard electronic components [6], [8], [9], and also simple chip integrated circuit [10], [11]. Since all of the linear elements (capacitors, resistor, and inductor) are readily available as two terminal devices, the main concern to realize the Chua's circuit is to design the nonlinear resistor (the Chua diode) with the characteristic delineated in Figure 2.5-b. Noting that the nonlinear resistor described therein is active, i.e., $v_R i_R = v_R g(v_R) \leq 0$, then active devices such as transistors or operational amplifiers should be used. Several implementation of the Chua diode already exist in literature, [8], [6], among which, we have chosen the realization depicted in Figure 2.9, to carry out all the simulations and experiments that will be investigated in chapter five.

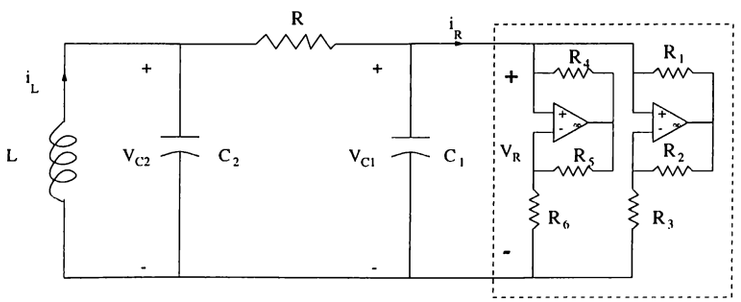

Figure 2.9: Practical implementation of Chua's circuit using two op-amps and six resistors to realize the Chua diode.

Figure 2.9 shows a practical implementation of Chua's circuit. The resistance values[2] chosen to implement the Chua diode lead to conductances: $Ga = -757\mu s$ and $Gb = -411\mu s$ if in addition, the following component values are chosen, $R = 1830\Omega$, $L = 18mH$, $C_1 = 10nF$ and $C_2 = 100nF$, the circuit will behave in a chaotic mode. The lf351 op-amps in this realization are modeled using Texas Instruments macro-model. Figure 2.10 shows a double-scroll Chua attractor obtained from the H-spice simulation of the circuit shown in Figure 2.9. Figure2.11 shows the time evolution of the state variables v_{C1} and its power spectrum density distributed on a normalized scale. It is clear that the chaotic signal is a broadband signal although Chua's circuit contains a harmonic oscillator of single sinusoidal frequency. The evolution of v_{C1} is an H-spice simulation output and the power spectrum density is a MATLAB Simulation output.

[2]R1=R2=220Ω, R3=2200Ω, R4=R5=22$k\Omega$ and R6=3300Ω. Op-amps are lf351, or equivalent.

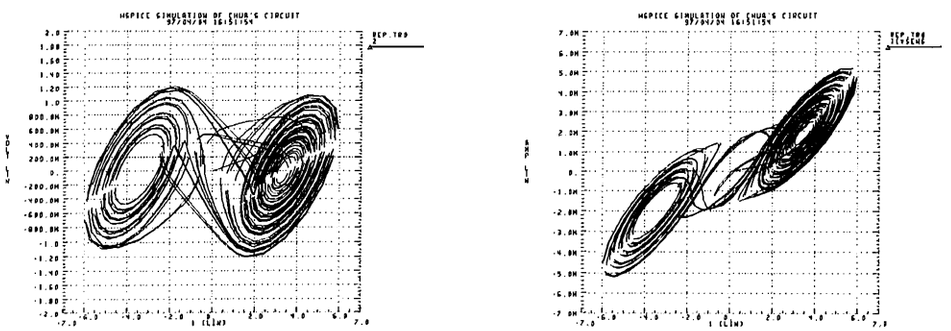

Figure 2.10: H-spice simulation of the Chua circuit. The first and second graphs represent: v_{C1}-signal vs v_{C2}-signal and v_{C1}-signal vs i_L-signal respectively.

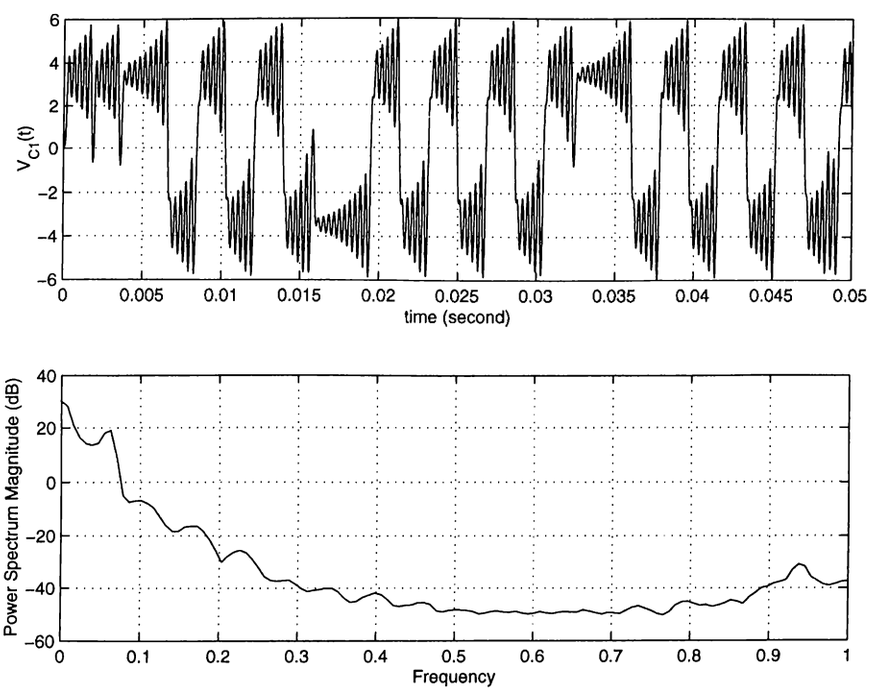

Figure 2.11: Time evolution of the state variables v_{C1} and its power spectrum density.

Chapter 3

Synchronizing Chaotic Systems: A Preview

"The ability to design synchronizing systems
in nonlinear and, especially, chaotic systems
may open interesting opportunities..."
T.L. Carroll and L.M. Pecora

Until last decades, most engineers were rather skeptical and reluctant to admit that chaotic behavior might have a practical use. Consequently, most research in this area focused on how to avoid chaos. But now a much more exciting motivation has emerged to exploit and harness the very special and peculiar features of chaotic behavior. In particular, self-synchronization of chaotic systems is an intriguing concept, and recently, has received considerable attention. It is believed that synchronization plays a crucial role in information processing, in living organisms, image processing [12], and neural networks [13]. Moreover, the synchronization property of chaotic circuits has revealed potential applications to secure communications, see e.g. [14] [15], [16] [17], [18] [19], [20] [21] [22].

Since the chaotic systems are deterministic, two trajectories that start from identical initial states will follow precisely the same paths through the state space. Nevertheless, the problem of obtaining two or more real chaotic circuits oscillating in a synchronized way is not a trivial task. As a matter of fact, it is impossible

in practice to construct two systems with identical parameters, let alone to start them from identical initial states. Due to the foregoing facts, two nearly identical systems starting from infinitesimally close initial states will have divergent orbits, and their time evolutions will be completely uncorrelated. However, recent work by Pecora and Carroll [23] [24] [25], Amritkar [26] [27] and others, have shown that it is possible to synchronize two chaotic systems so that their trajectories remain close.

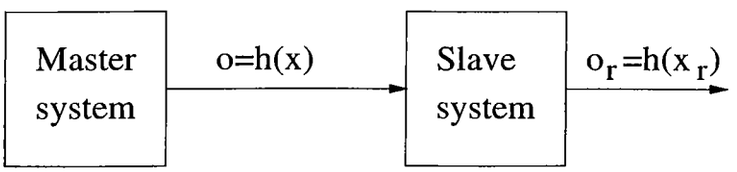

Figure 3.1: Master-slave configuration.

In this chapter, we consider a set-up where a *master system* drives a *slave system* in order to impose its waveforms. This situation is depicted schematically in Figure 3.1. Both systems should be thought of as being chaotic. In general, the slave system is nothing but a duplication of the master system, except that it has an additional control input (non-autonomous) which is either driven directly with the transmitted signal $o(t)$, as shown in Figure 3.1, or it is driven by some error signal.

Should the transmitted signal $o(t)$ be appropriately chosen, the output $o_r(t)$ of the slave system will be forced to copy the waveform of the driving signal $o(t)$. Assuming the initial states of the two systems to be different, and knowing that the evolution of a chaotic system depends on its initial state, we cannot expect $o_r(t)$ to be identical to $o(t)$. Only in the limit, the influence of the initial state can be expected to fade away. This justifies the following definition, see e.g. [20]:

Definition 3.1 *The slave system synchronizes with the master system if*

$$\lim_{t\to\infty} \|\mathbf{o}(t) - \mathbf{o}_r(t)\| = 0$$

for any combination of initial states of the master and the slave systems.

Next, we shall show five methods to synchronize chaotic systems, namely

1. by decomposition into subsystems
2. by linear mutual coupling
3. by linear feedback
4. by the inverse system
5. by observer design

3.1 Synchronization by Decomposition Into Subsystems

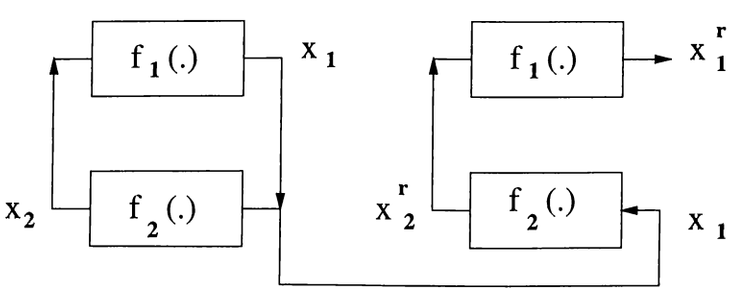

Figure 3.2: Master-slave set-up for synchronization by decomposition into subsystems.

The idea of synchronization by decomposition into subsystems has first been proposed by Pecora and Carroll [23]. This synchronization scheme applies to systems that are drive-decomposable. A dynamical system is called drive-decomposable if it can be partitioned into two subsystems that are coupled so that the behavior of the second (called the response subsystem) depends on that of the first, but the behavior of the first (called the drive subsystem) is independent of that of the second.

To construct a drive-decomposable system, an n-dimensional, autonomous, continuous-time dynamical system

$$\dot{\mathbf{x}} = \mathbf{f}(\mathbf{x}), \quad \mathbf{x}(0) = \mathbf{x}_0 \tag{3.1}$$

where $\mathbf{x} = (x_1, x_2, \ldots, x_n)^T$ and $\mathbf{f}(\mathbf{x}) = [f_1(\mathbf{x}), f_2(\mathbf{x}), \ldots f_n(\mathbf{x})]^T$, is first partitioned into two subsystems

$$\dot{\mathbf{x}}_1 = \mathbf{f_1}(\mathbf{x_1}, \mathbf{x_2}), \quad \mathbf{x_1}(0) = \mathbf{x}_{1_0} \tag{3.2}$$

$$\dot{\mathbf{x}}_2 = \mathbf{f_2}(\mathbf{x_1}, \mathbf{x_2}), \quad \mathbf{x_2}(0) = \mathbf{x}_{2_0} \tag{3.3}$$

where $\mathbf{x_1} = (x_1, x_2, \ldots, x_m)^T, \quad \mathbf{x_2} = (x_{m+1}, x_{m+2}, \ldots, x_n)^T,$

$$\mathbf{f_1}(\mathbf{x_1}, \mathbf{x_2}) = \begin{pmatrix} f_1(\mathbf{x_1}, \mathbf{x_2}) \\ f_2(\mathbf{x_1}, \mathbf{x_2}) \\ \vdots \\ f_m(\mathbf{x_1}, \mathbf{x_2}) \end{pmatrix}$$

and

$$\mathbf{f_2}(\mathbf{x_1}, \mathbf{x_2}) = \begin{pmatrix} f_{m+1}(\mathbf{x_1}, \mathbf{x_2}) \\ f_{m+2}(\mathbf{x_1}, \mathbf{x_2}) \\ \\ f_n(\mathbf{x_1}, \mathbf{x_2}) \end{pmatrix}$$

An identical $(n-m)$-dimensional copy of the second subsystem, with $\mathbf{x}_2^r$ as state variable and $\mathbf{x_1}$ as input, is appended to form the following $(2n-m)$-dimensional coupled drive-response system:

$$\dot{\mathbf{x}}_1 = \mathbf{f_1}(\mathbf{x_1}, \mathbf{x_2}) \ , \quad \mathbf{x_1}(0) = \mathbf{x}_{1_0} \tag{3.4}$$

$$\dot{\mathbf{x}}_2 = \mathbf{f_2}(\mathbf{x_1}, \mathbf{x_2}) \ , \quad \mathbf{x_2}(0) = \mathbf{x}_{2_0} \tag{3.5}$$

$$\dot{\mathbf{x}}_2^r = \mathbf{f_2}(\mathbf{x_1}, \mathbf{x_2^r}) \ , \quad \mathbf{x}_2^r(0) = \mathbf{x}_{2_0}^r \tag{3.6}$$

The n-dimensional dynamical system defined by (3.4) and (3.5) is called the drive system and (3.6) is called the response subsystem.

Note that the second drive subsystem (3.5) and the response subsystem (3.6) lie in state space of dimension $\mathbf{R}^{(n-m)}$ and have identical vector field $\mathbf{f_2}$ and input $\mathbf{x_1}$.

Consider a trajectory $\mathbf{x}_2^r(t)$ of (3.6) that originates from an initial state $\mathbf{x}_{2_0}^r$ "close" to $\mathbf{x}_{2_0}$. We may think of $\mathbf{x}_2(t)$ as a perturbation of $\mathbf{x}_2^r(t)$. In particular, define the error $\mathbf{e_x}(t) = \mathbf{x}_2(t) - \mathbf{x}_2^r(t)$. The trajectory $\mathbf{x}_2^r(t)$ approaches $\mathbf{x}_2(t)$ asymptotically (synchronizes) if according to definition 3.1 $\|e_\mathbf{x}\| \to 0$ as $t \to \infty$. Equivalently, the response subsystem asymptotically tends to $\mathbf{x}_2(t)$ when it is driven with $\mathbf{x}_1(t)$.

Example 3.1 *If we consider*

$$\dot{\mathbf{x}}_2 = g(\mathbf{x}_1) + \mathbf{A}\mathbf{x}_2$$

$$\dot{\mathbf{x}}_2^r = g(\mathbf{x}_1) + \mathbf{A}\mathbf{x}_2^r$$

where $\mathbf{A}$ *is a stable matrix, then*

$$\dot{e}_x = \mathbf{A}e_x$$

hence $\|e_x\| \to 0$ *exponentially fast.* □

The synchronization of the response subsystem may be determined by examining the linearization of the vector field along the response signal. The linearized response subsystem is governed by

$$\dot{\mathbf{x}}_l = \mathbf{D}_{x_l}\mathbf{f_2}(\mathbf{x_1}(t), \mathbf{x_2^r})\mathbf{x}_l, \quad \mathbf{x}_l(0) = \mathbf{x}_{l_0} \tag{3.7}$$

where $\mathbf{D}_{x_l}\mathbf{f_2}(\mathbf{x_1}(t), \mathbf{x_2^r})$ denotes the partial derivatives of the vector field $\mathbf{f_2}$ of the response subsystem with respect to $\mathbf{x}_2^r$. This is a linear time-varying system whose state transition matrix $\Phi(t, t_0)$ maps a point $\mathbf{x}_l(t_0)$ into $\mathbf{x}_l(t)$. Thus

$$\mathbf{x}_l(t) = \Phi(t, 0)\mathbf{x}_{l_0} \tag{3.8}$$

Note that Φ is a linear operator. The conditional Lyapunov exponents $\lambda_i(\mathbf{x}_{1_0}, \mathbf{x}_{2_0})$ (hereafter denoted CLE) are defined by

$$\lambda_i(\mathbf{x}_{1_0}, \mathbf{x}_{2_0}) = \lim_{t\to\infty} \frac{1}{t}\, ln\ \sigma_i[\Phi(t, 0)], \quad i = 1, 2, \ldots, (n - m) \tag{3.9}$$

whenever the limit exists, and where σ_i denotes the ith singular value of the transition matrix $\Phi(t,0)$. The term conditional refers to the fact that the exponents depends explicitly on the trajectory of the drive system. Based on the CLE, Pecora and Caroll proved the following theorem, see [28]

Theorem 3.1 *The trajectories* $\mathbf{x_2}(t)$ *and* $\mathbf{x}_2^r(t)$ *will synchronize only if the CLE's of the response system are all negative.*

Remark 3.1 *Note that this is a necessary but not sufficient condition for synchronization. However, if the response and second drive subsystems are identical and the initial conditions* $\mathbf{x}_{2_0}$ *and* $\mathbf{x}_{2_0}^r$ *are sufficiently close, and the CLE's of (3.6) are all negative, synchronization will occur. On the other hand, if the systems are not identical, (in our work we do not assume this case) synchronization might not occur, even if all of the CLE's are negative.*

Although we have described it only for an autonomous continuous-time system, the drive response technique may also be applied for synchronizing non-autonomous and discrete-time circuits, see [29] [30] [31].

The drive-response concept may be extended to the case where a dynamical system can be partitioned into more than two parts. A simple two-level drive-response cascade is constructed as follows. Divide the dynamical system

$$\dot{\mathbf{x}} = \mathbf{f}(\mathbf{x}), \quad \mathbf{x}(0) = \mathbf{x}_0 \tag{3.10}$$

into three parts:

$$\dot{\mathbf{x}}_1 = \mathbf{f_1}(\mathbf{x_1}, \mathbf{x_2}, \mathbf{x_3}), \quad \mathbf{x_1}(0) = \mathbf{x}_{1_0} \tag{3.11}$$

$$\dot{\mathbf{x}}_2 = \mathbf{f_2}(\mathbf{x_1}, \mathbf{x_2}, \mathbf{x_3}), \quad \mathbf{x_2}(0) = \mathbf{x}_{2_0} \tag{3.12}$$

$$\dot{\mathbf{x}}_3 = \mathbf{f_3}(\mathbf{x_1}, \mathbf{x_2}, \mathbf{x_3}), \quad \mathbf{x_3}(0) = \mathbf{x}_{3_0} \tag{3.13}$$

Now construct an identical copy of the subsystems corresponding to (3.12) and (3.13) with $\mathbf{x_1}(t)$ as input:

$$\dot{\mathbf{x}}_2^r = \mathbf{f_2}(\mathbf{x_1}, \mathbf{x_2^r}, \mathbf{x_3^r}), \quad \mathbf{x}_2^r(0) = \mathbf{x}_{2_0}^r \tag{3.14}$$

$$\dot{\mathbf{x}}_3^r = \mathbf{f_3}(\mathbf{x_1}, \mathbf{x_2^r}, \mathbf{x_3^r}), \quad \mathbf{x}_3^r(0) = \mathbf{x}_{3_0}^r \tag{3.15}$$

If all of the CLE's of the driven subsystem composed of (3.14) and (3.15) are negative then, after the transient decays, $\lim_{t\to\infty}(\mathbf{x}_2^r(t) - \mathbf{x}_2(t)) = 0$ and $\lim_{t\to\infty} \mathbf{x}_3^r(t) - \mathbf{x}_3(t)) = 0$.

Proceeding one step further, we reproduce subsystem (3.11):

$$\dot{\mathbf{x}}_1^r = \mathbf{f_1}(\mathbf{x_1^r}, \mathbf{x_2^r}, \mathbf{x_3^r}), \quad \mathbf{x}_1^r(0) = \mathbf{x}_{1_0}^r \tag{3.16}$$

Similarly, if all of the conditional Lyapunov exponents of (3.16) are negative, then using Theorem 3.1 and Remark 3.1, we expect $\mathbf{x}_1^r(t)$ to converge to $\mathbf{x}_1(t)$ and continue to remain in its steps.

In the following two sub-sections, we shall apply this scheme on some concrete dynamical systems, namely: Lorenz system and Chua's circuit.

3.1.1 Synchronization of Lorenz System

We consider the following well-known Lorenz system as the drive system:

$$\dot{x} = \sigma(y - x) \ , \tag{3.17}$$

$$\dot{y} = -xz + rx - y \ , \tag{3.18}$$

$$\dot{z} = xy - bz \ . \tag{3.19}$$

We choose the parameters σ, r and b so that the system (3.17)-(3.19) is in the chaotic regime as $\sigma = 10$, $r = 20$, $b = 1$. The solution $x(t)$ of (3.17)-(3.19) will be used to synchronize the solutions of the following response system,

$$\dot{x}_r = \sigma(y_r - x_r) \ , \tag{3.20}$$

$$\dot{y}_r = -xz_r + rx - y_r \ , \tag{3.21}$$

$$\dot{z}_r = xy_r - bz_r \ . \tag{3.22}$$

We first note the following simple fact :

Lemma 3.1 *Consider the following system :*

$$\dot{w} = Aw + f(t) \quad , \tag{3.23}$$

where $w \in \mathbf{R}^n$, $A \in \mathbf{R}^{n\times n}$, $f(\cdot) : \mathbf{R}_+ \to \mathbf{R}^n$ is a differentiable function. Assume that the matrix A is Hurwitz-stable (i.e. all eigenvalues are in the open left half of the complex plane), and that $f(t)$ decreases exponentially to zero, i.e. for some $M_1 > 0$ and $\alpha_1 > 0$, the following holds :

$$\|f(t)\| \leq M_1 e^{-\alpha_1 t} \ , \quad t \geq 0 \quad . \tag{3.24}$$

Then, for any $w(0) \in \mathbf{R}^n$, the solution $w(t)$ of (3.23) also decays exponentially to zero.

Proof : The solution $w(t)$ of (3.23) can be written as :

$$w(t) = e^{At}w(o) + \int_0^t e^{A(t-\tau)}f(\tau)d\tau \quad . \tag{3.25}$$

Since A is Hurwitz stable, there exist constants $M_2 > 0$ and $\alpha_2 > 0$ such that the following holds :

$$\|e^{At}\| \leq M_2 e^{-\alpha_2 t} \quad , \tag{3.26}$$

where $\|\cdot\|$ in (3.26) is now the induced matrix norm, see e.g. [32]. Hence, the first term in the right hand side of (3.25) clearly decays to zero exponentially fast. For the second term, note that

$$\| \int_0^t e^{A(t-\tau)}f(\tau)d\tau\| \leq M_1 M_2 e^{-\alpha_2 t} \int_0^t e^{(\alpha_2-\alpha_1)\tau}d\tau \quad , \tag{3.27}$$

where we used (3.24) and (3.26). Without loss of generality we may assume that $\alpha_1 \neq \alpha_2$, for otherwise by slightly decreasing α_1 and/or α_2 one can easily find values for α_1 and α_2 such that $\alpha_1 \neq \alpha_2$ and both (3.24) and (3.26) are satisfied. Then, simple integration shows that the second term in the right hand side of (3.25), and hence also $w(t)$, decay exponentially to zero. □

To prove the synchronization, let us define the synchronization error terms as follows :

$$e_x = x - x_r \quad , \quad e_y = y - y_r \quad , \quad e_z = z - z_r \quad , \tag{3.28}$$

Lemma 3.2 *For any $e_x(0)$, $e_y(0)$, $e_z(0)$, the errors defined by (3.28) associated with the systems (3.17)-(3.19) and (3.20)-(3.22) decay exponentially to zero.*

Remark 3.2 *The synchronization of (3.17)-(3.19) with (3.21)-(3.22) (i.e for e_y and e_z) could be found in [25]. Asymptotic synchronization of (3.17)-(3.19) and (3.20)-(3.22) can be found in [18]. Below it will be emphasized that the synchronization is in fact exponential. This analysis is based on Lemma 2 and a Lyapunov function, different than the one used in [18],* □

Proof : By using (3.18)-(3.19) and (3.21)-(3.22) we obtain :

$$\dot{e}_y = -xe_z - e_y \quad , \tag{3.29}$$

$$\dot{e}_z = xe_y - be_z \quad . \tag{3.30}$$

Let us define the Lyapunov function V as :

$$V = \frac{1}{2}e_y^2 + \frac{1}{2}e_z^2 \quad . \tag{3.31}$$

Simple differentiation of V along the solutions of (3.29)-(3.30) results in :

$$\dot{V} = -e_y^2 - be_z^2 \quad . \tag{3.32}$$

Since $b > 0$, this shows that all solutions of (3.29)-(3.30) globally asymptotically decay to zero, see TheoremA.2. Moreover, from (3.31) and (3.32) it easily follows that $V(t) \leq e^{-kt}V(0)$, where $k = 2\min\{1, b\}$. Moreover, since $b = 1$, we have $\dot{V} = -2V$, which implies that $V(t) = e^{-2t}V(0)$, hence the errors $e_y(t)$ and $e_z(t)$ in fact decay exponentially to zero. This in particular implies that $\mid e_y(t) \mid \leq e^{-t}\|e(0)\|$ where $\|e(t)\| = \sqrt{e_x^2(t) + e_y^2(t) + e_z^2(t)}$. Then, using (3.17) and (3.20) we obtain :

$$\dot{e}_x = -\sigma e_x + \sigma e_y \quad . \tag{3.33}$$

Since $\sigma > 0$ and e_y decays exponentially to zero, it follows from Lemma 3.1 that e_x also decays exponentially to zero. The solution of (3.33) is given as

$$e_x(t) = e^{-\sigma t}e_x(0) + \int_0^t \sigma e^{-\sigma(t-\tau)}e_y(\tau)d\tau \quad .$$

Hence, by taking norms, using the facts given above and $\sigma > 1$, we obtain

$$\|e(t)\| \leq \sqrt{2 + \frac{8\sigma^2}{(\sigma-1)^2}} e^{-t} \|e(0)\| \ ,$$

which implies that the synchronization is exponentially fast. □

Remark 3.3 *In [25], depending on the synchronization signal, various drive-response systems have been proposed. In particular, for Lorenz system, instead of (3.20)-(3.22), the following response system can also be used :*

$$\dot{x}_r = \sigma(y - x_r) \ , \tag{3.34}$$

$$\dot{y}_r = -x_r z_r + r x_r - y_r \ , \tag{3.35}$$

$$\dot{z}_r = x_r y - b z_r \ . \tag{3.36}$$

where, this time $y(t)$ is used for synchronization. It can easily be shown that the error signals defined by (3.28) also decay exponentially to zero. □

3.1.2 Synchronization of Chua's Circuit

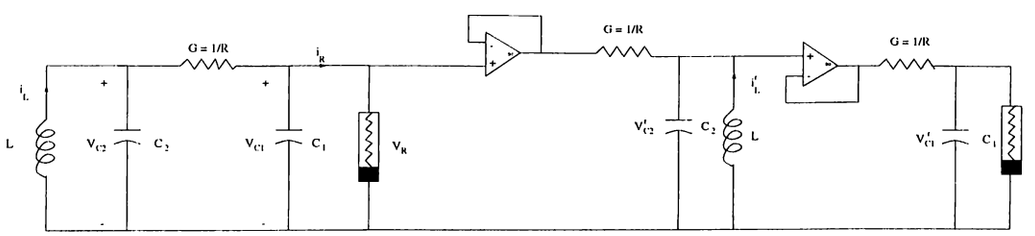

Figure 3.3: Synchronization of two Chua's circuits.

Now, let's consider the Chua's circuit as the chaotic dynamical system. It has been shown in the previous chapter that the Chua's circuit is governed by the following state equations:

$$\frac{dv_{C1}}{dt} = \frac{G}{C_1}(v_{C2} - v_{C1}) - \frac{1}{C_1} f(v_{C1}) \ , \tag{3.37}$$

$$\frac{dv_{C2}}{dt} = \frac{G}{C_2}(v_{C1} - v_{C2}) + \frac{1}{C_2} i_L \ , \tag{3.38}$$

$$\frac{di_L}{dt} = -\frac{1}{L} v_{C2} \ . \tag{3.39}$$

Let the circuit parameters be as indicated previously, hence, the circuit is behaving in the chaotic regime. The voltage signal $v_{C1}(t)$ of the drive system (3.37)-(3.39) will be used to synchronize the response system having the following governing equations, (where the superscript r stands for response):

$$\frac{dv_{C1}^r}{dt} = \frac{G}{C_1}(v_{C2}^r - v_{C1}^r) - \frac{1}{C_1}f(v_{C1}^r) \ , \tag{3.40}$$

$$\frac{dv_{C2}^r}{dt} = \frac{G}{C_2}(v_{C1} - v_{C2}^r) + \frac{1}{C_2}i_L^r \ , \tag{3.41}$$

$$\frac{di_L^r}{dt} = -\frac{1}{L}v_{C2}^r \ . \tag{3.42}$$

Figure 3.3 depicts the master-slave configuration described by the drive and the response systems, (3.37)-(3.42). In order to show that both systems will synchronize, let's define the corresponding error terms as follows:

$$e_{v_{C1}} = v_{C1} - v_{C1}^r \ , \ e_{v_{C2}} = v_{C2} - v_{C2}^r \ , \ e_{i_L} = i_L - i_L^r \ , \tag{3.43}$$

Lemma 3.3 *For any $e_{v_{C1}}(0)$, $e_{v_{C2}}(0)$, $e_{i_L}(0)$, the errors defined by (3.43) associated with the systems (3.37)-(3.39) and (3.40)-(3.42) decay exponentially to zero.*

Proof : By using (3.38)-(3.39) and (3.41)-(3.42) we obtain :

$$\dot{e}_{v_{C2}} = -\frac{1}{RC_2}e_{v_{C2}} + \frac{1}{C_2}e_{i_L} \ , \tag{3.44}$$

$$\dot{e}_{i_L} = -\frac{1}{L}e_{v_{C2}} \ . \tag{3.45}$$

We can also write equations (3.44) and (3.45) in matrix form

$$\dot{\mathbf{e}}_z = \mathbf{A}\mathbf{e}_z \ . \tag{3.46}$$

where $\mathbf{A}$ is given by:

$$A = \begin{bmatrix} -\frac{1}{RC_2} & \frac{1}{C_2} \\ -\frac{1}{L} & 0 \end{bmatrix} ,$$

and $\mathbf{e}_z = (e_{v_{C2}}, e_{i_L})^T$. Now the general solution of (3.44) and (3.45) is given by:

$$\mathbf{e}_z(t) = e^{\mathbf{A}t}\mathbf{e}_z(t_0) \ . \tag{3.47}$$

In fact, we can make use of the values of the components, to show that the matrix $\mathbf{A}$ is Hurwitz-stable, thus

$$\|\mathbf{e}_z(t)\| \leq Me^{-\alpha(t-t_0)}\|\mathbf{e}_z(t_0)\| \tag{3.48}$$

for some $M > 0$ and $\alpha > 0$, hence the system defined by (3.47) is globally asymptotically stable, i.e.

$$\mathbf{e}_z(t) = e^{\mathbf{A}t}\mathbf{e}_z(t_0) \to 0 \quad as \quad t \to \infty \ .$$

Since the parameters G and C_1 are positive, also the function $f(.)$ is bounded in terms of its argument, and $e_{v_{C2}}(t)$ decays to zero exponentially fast, it follows from Lemma 3.1 that $e_{v_{C1}}(t)$ also decays to zero. □

3.2 Synchronization by Linear Mutual Coupling

This is a very simple technique to synchronize two dynamical systems described by the following differential equation:

$$\dot{\mathbf{x}}_i = \mathbf{f_i}(\mathbf{x_1}, \mathbf{x_2}), \quad \mathbf{x_i}(0) = \mathbf{x}_{i_0}, \quad i = 1, 2.$$

it is merely a linear mutual coupling of the form

$$\dot{\mathbf{x}}_1 = \mathbf{f}_1(\mathbf{x}_1, \mathbf{x}_2) + \mathbf{K}(\mathbf{x}_2 - \mathbf{x}_1), \quad \mathbf{x}_1(0) = \mathbf{x}_{1_0} \tag{3.49}$$

$$\dot{\mathbf{x}}_2 = \mathbf{f}_2(\mathbf{x}_1, \mathbf{x}_2) + \mathbf{K}(\mathbf{x}_1 - \mathbf{x}_2), \quad \mathbf{x}_2(0) = \mathbf{x}_{2_0} \tag{3.50}$$

where $\mathbf{x_1}, \mathbf{x_2} \in \mathbf{R}^n$ and $\mathbf{K} = diag(k_{11}, k_{22}, \ldots, k_{nn})^T$. Here, the synchronization problem may be stated as follows: find $\mathbf{K}$ such that

$$\lim_{t\to\infty} \|\mathbf{x_1}(t) - \mathbf{x_2}(t)\| = 0$$

In general it is difficult to prove that synchronization occurs, unless an appropriate Lyapunov function of the error system $\mathbf{e}(t) = \mathbf{x_1}(t) - \mathbf{x_2}(t)$ can be found. However, several examples exist in the literature where mutually coupled chaotic systems synchronize over particular ranges of parameters. Next, we will state an example of synchronization via mutual coupling technique. Moreover, we will provide a proof of the synchronization by using a Lyapunov function.

Example: Mutually Coupled Chua's Circuit

Consider a linear mutual coupling of two Chua's circuit as depicted in Figure 3.4.

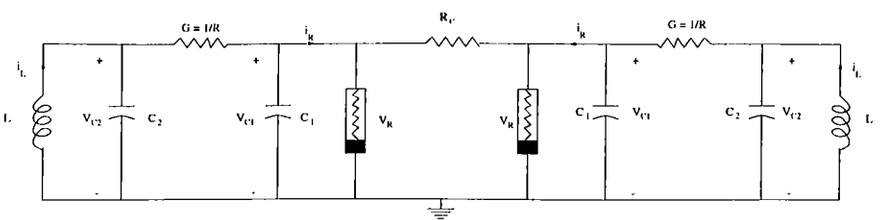

Figure 3.4: Synchronization of two Chua's circuits by means of resistive coupling.

The system under consideration is:

$$\begin{aligned}
\frac{dv_{C1}}{dt} &= \frac{G}{C_1}(v_{C2} - v_{C1}) - \frac{1}{C_1}f(v_{C1}) + \frac{G_C}{C_1}(v^r_{C1} - v_{C1}) \ , \\
\frac{dv_{C2}}{dt} &= \frac{G}{C_2}(v_{C1} - v_{C2}) + \frac{1}{C_2}i_L \ , \\
\frac{di_L}{dt} &= -\frac{1}{L}v_{C2} \ , \\
\frac{dv^r_{C1}}{dt} &= \frac{G}{C_1}(v^r_{C2} - v^r_{C1}) - \frac{1}{C_1}f(v^r_{C1}) + \frac{G_C}{C_1}(v_{C1} - v^r_{C1}) \ , \\
\frac{dv^r_{C2}}{dt} &= \frac{G}{C_2}(v^r_{C1} - v^r_{C2}) + \frac{1}{C_2}i^r_L \ , \\
\frac{di^r_L}{dt} &= -\frac{1}{L}v^r_{C2} \ .
\end{aligned}$$

and the error system is as follows

$$\dot{e}_{v_{C1}} = \frac{G}{C_1}(e_{v_{C2}} - e_{v_{C1}}) - \frac{1}{C_1}[f(v_{C1}) - f(v^r_{C1})] - \frac{2G_C}{C_1}e_{v_{C1}} \ , \qquad (3.51)$$

$$\dot{e}_{v_{C2}} = \frac{G}{C_2}(e_{v_{C1}} - e_{v_{C2}}) + \frac{1}{C_2}e_{i_L} \ , \tag{3.52}$$

$$\dot{e}_{i_L} = -\frac{1}{L}e_{v_{C2}}. \tag{3.53}$$

Let us define the Lyapunov function V as:

$$V = \frac{C_1}{2}e_{v_{C1}}^2 + \frac{C_2}{2}e_{v_{C2}}^2 + \frac{L}{2}e_{i_L}^2 \ .$$

taking the derivative of V along the solutions of (3.51)-(3.53) results in:

$$\dot{V} = -G(e_{v_{C1}} - e_{v_{C2}})^2 - 2G_C e_{v_{C1}}^2 - e_{v_{C1}}[f(v_{C1}) - f(v_{C1}^r)] \ .$$

Knowing that

$$-e_{v_{C1}}|f(v_{C1}) - f(v_{C1}^r)| \leq |G_a||e_{v_{C1}}|^2 \ ,$$

then

$$\dot{V} \leq -G(e_{v_{C1}} - e_{v_{C2}})^2 - (2G_C - |G_a|)e_{v_{C1}}^2 \ , \tag{3.54}$$

if the coupling parameter is chosen such that $(2G_C - |G_a|) \geq 0$ then $\dot{V}$ is negative, hence the error system is uniformly asymptotically stable. Therefore using Theorem A.1 and Theorem A.3 in Appendix A we may conclude that the synchronization is exponentially fast.

3.3 Synchronization by Linear Feedback

The point of view of this method is typical for automatic control. We consider two identical systems as master and slave, compare their outputs and use the difference to control the slave system, see Figure 3.5. This approach has been used in [33] [34] [35].

Consider an autonomous n-dimensional dynamical system evolving via the evolution equation

$$\dot{\mathbf{x}} = \mathbf{f}(\mathbf{x}, \mu) \ , \tag{3.55}$$

where $\mathbf{x}=(x_1, \ldots, x_n)^T$ and $\mathbf{f}(\mathbf{x}, \mu) = (\mathbf{f}_1(\mathbf{x}_1, \mu), \ldots, \mathbf{f}_n(\mathbf{x}_n, \mu))^T$ are n-dimensional vectors and the function $\mathbf{f}$ depends on the set of parameters $\mu = (\mu_1, \ldots, \mu_k)^T$. Parameters μ are such that the system shows a chaotic behavior.

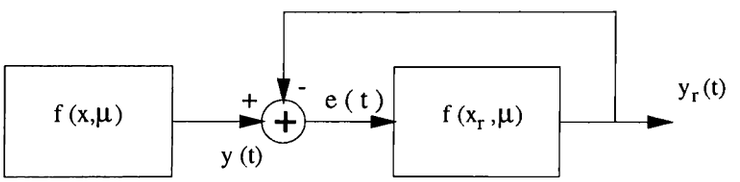

Figure 3.5: Master-slave set-up for synchronization by linear feedback.

If the error signal controls the state variables, the state equations of the whole system of Figure 3.5 become

$$\dot{\mathbf{x}} = \mathbf{f}(\mathbf{x}, \mu) \tag{3.56}$$

$$\mathbf{y}(t) = \mathbf{C}\mathbf{x}(t) \tag{3.57}$$

$$\dot{\mathbf{x}}_r = \mathbf{f}(\mathbf{x}_r, \mu) + \mathbf{K}\mathbf{e}(t) \tag{3.58}$$

$$\mathbf{y}_r(t) = \mathbf{C}\mathbf{x}_r(t) \tag{3.59}$$

$$\mathbf{e}(t) = \mathbf{y}(t) - \mathbf{y}_r(t) \tag{3.60}$$

Our objective is to chose the feedback control matrix $\mathbf{K}$ so that the state variables $\mathbf{x}_r(t)$ of the slave system are forced onto the desired state variable $\mathbf{x}(t)$ of the master system and consequently $\|\mathbf{e}(t)\| = \|\mathbf{y}(t) - \mathbf{y}_r(t)\| \to 0$ as $t \to \infty$.

Again, if the master and the slave system started from exactly the same initial conditions then at all times, $\mathbf{x}(t) = \mathbf{x}_r(t)$, $\mathbf{y}(t) = \mathbf{y}_r(t)$, and $\|\mathbf{e}(t)\| = 0$. It, is indeed, impossible to reproduce the same starting conditions. Nevertheless, the system described by (3.56)-(3.60) can reach synchronization under certain conditions.

The linear feedback approach can be applied successfully to Chua's circuit. The governing equations of Chua's circuit can be written in the following form:

$$\dot{\mathbf{x}} = \mathbf{A}\mathbf{x} + \mathbf{b}f(x_1), \quad \mathbf{y} = \mathbf{C}\mathbf{x}\ , \tag{3.61}$$

where

$$A = \begin{bmatrix} -\frac{G}{C_1} & \frac{G}{C_1} & 0 \\ \frac{G}{C_2} & -\frac{G}{C_2} & +\frac{1}{C_2} \\ 0 & -\frac{1}{L} & 0 \end{bmatrix},$$

and

$$f(x) = \begin{cases} G_b x + (G_b - G_a)E & if \quad x < -E \\ G_a x & if \quad -E \leq x \leq E \\ G_b x + (G_a - G_b)E & if \quad x > E \end{cases} \tag{3.62}$$

$\mathbf{b} = (1,0,0)^T$, $\mathbf{y}$ is the output of the system, and $\mathbf{x} = (x_1, x_2, x_3)^T = (v_{C1}, v_{C2}, i_L)^T$. The slave system is described by the state equation

$$\dot{\mathbf{x}}_r = \mathbf{A}\mathbf{x}_r + \mathbf{b}f(x_{1r}) + \mathbf{KC}(\mathbf{x} - \mathbf{x}_r), \quad \mathbf{y}_r = \mathbf{C}\mathbf{x}_r \ . \tag{3.63}$$

Subtracting (3.63) from (3.61) we get the synchronization error on the state variables $\mathbf{e}(t) = \mathbf{x}(t) - \mathbf{x}_r(t)$

$$\dot{e} = (\mathbf{A} - \mathbf{KC})\mathbf{e} + \mathbf{b}(f(x_1) - f(x_{1r})) \tag{3.64}$$

Note that the right hand side of (3.64) can be interpreted as a homogeneous part and an excitation part. The excitation is given by the difference between the two piecewise linear functions $f(x_1)$ and $f(x_{1r})$.

The selection of $\mathbf{y} = x_1 = v_{C1}$ (i.e., $\mathbf{C} = (1,0,0)$) makes the pair $(\mathbf{C}, \mathbf{A})$ observable, hence by an appropriate choice of the control $\mathbf{K}$, one may obtain a stable matrix $\mathbf{A} - \mathbf{KC}$, since in addition we know that $-e_{x1}|f(x_1) - f(x_{1r})| \leq |G_a||e_{x1}|$, then by appropriate choice of $\mathbf{K}$ we may obtain synchronization, see [36], [37].

Although, we have shown that synchronization is achieved when the feedback control is applied only to the state variable, it is our belief that, feedback control may also be applied to control the parameters μ in order to avoid significant parameter mismatch [27].

3.4 Synchronization by The Inverse System

For this method the setup is somewhat different. Instead of using, as the basic building block, an autonomous system with chaotic behavior, we start with a master system that is excited by an input signal $s(t)$ and produces an output signal $y(t)$. The signal $s(t)$ can be thought of as having a rather regular waveform (e.g., the message modulated by a harmonic frequency or the message to be transmitted itself), whereas the signal $y(t)$ is intended to be chaotic.

The signal $y(t)$, inherently bearing the message, drives a slave system that is the inverse of the master system in the sense that, starting from identical initial conditions, its output is identical to the input of the master system, i.e., $s_r(t) = s(t)$ see Figure 3.6.

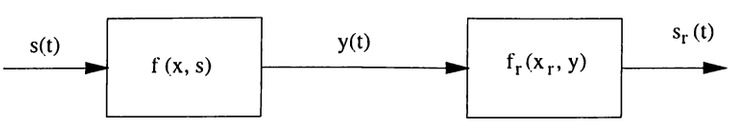

Figure 3.6: Master-slave set-up for synchronization by the inverse system.

The state equations for the system depicted above have the form

$$\dot{\mathbf{x}} = \mathbf{f}(\mathbf{x}, \mathbf{s}) \tag{3.65}$$

$$\mathbf{y} = \mathbf{g}(\mathbf{x}, \mathbf{s}) \tag{3.66}$$

$$\dot{\mathbf{x}}_r = \mathbf{f}_r(\mathbf{x}_r, \mathbf{y}) \tag{3.67}$$

$$\mathbf{s}_r = \mathbf{h}(\mathbf{x}_r, \mathbf{y}) \tag{3.68}$$

At first sight, it might seem a formidable task to find an inverse for a nonlinear dynamical system. In literature, however, there are evident candidates for inverse systems. To make things clearer, we shall present a relevant example of chaotic synchronization by the inverse system, see also [38] [39].

Let us consider a second-order non-autonomous system having the following state space representation:

$$\dot{x} = y \tag{3.69}$$

$$\dot{y} = -\alpha y + x - x^3 + s(t) \tag{3.70}$$

where

$$s(t) = m(t) + f(t) = m(t) + E\cos\omega_0 t$$

and $m(t)$ is nothing but the message to be transmitted. Note that the system described by (3.69)-(3.70) is known to be chaotic if the parameters are chosen properly. Let us assume that the signal $x(t)$ is sent to the receiver defined as:

$$\dot{x}_r = y_r \ , \tag{3.71}$$

$$\dot{y}_r = -\alpha y_r + x - x^3 \ . \tag{3.72}$$

If we subtract (3.71)-(3.72) from (3.69)-(3.70), then we obtain

$$\dot{e}_x = e_y \ , \tag{3.73}$$

$$\dot{e}_y = -\alpha e_y + s(t) \ , \tag{3.74}$$

where

$$\dot{e}_x = x - x_r, \quad \text{and} \quad \dot{e}_y = y - y_r$$

From (3.73) and (3.74) we obtain:

$$s(t) = \dot{e}_y + \alpha e_y = \ddot{e}_x + \alpha \dot{e}_x \tag{3.75}$$

Now since e_x is measurable, then to recover $s(t)$ we just need to differentiate e_x and $\dot{e}_x$, then apply them to (3.75). The recovering equation (3.75) seems quite simple, since the receiver needs only some linear operations such as differentiation and addition. In practice, however, the differentiation is considered to be an unstable operation which might doom the system.

3.5 Observer Based Synchronization

This a new technique to synchronize chaotic systems. It has been first proposed in [36] and [37]. In this approach, once the drive system is given, the response system could be chosen in the observer form, and the drive signal should be chosen accordingly so that the drive system satisfies certain conditions. Under some mild

conditions, local or global synchronization of drive and observer systems can be guaranteed. Hence this synchronization scheme offers a systematic procedure, independent of the choice of the drive system.

Consider the nonlinear system given below

$$\dot{\mathbf{x}} = \mathbf{A}\mathbf{x} + \mathbf{g}(\mathbf{x}) \quad , \quad \mathbf{o} = \mathbf{C}\mathbf{x} \quad , \tag{3.76}$$

where $\mathbf{A} \in \mathbf{R}^{n\times n}$ and $\mathbf{C} \in \mathbf{R}^{M\times n}$ are constant matrices, $\mathbf{g} : \mathbf{R}^n \rightarrow \mathbf{R}^n$ is a differentiable function. Assume that $\mathbf{g}$ satisfies the following Lipschitz condition:

$$\|\mathbf{g}(\mathbf{x_1}) - \mathbf{g}(\mathbf{x_2})\| \leq k\|\mathbf{x_1} - \mathbf{x_2}\| \quad , \quad \forall \mathbf{x_1},\ \mathbf{x_2} \in \mathbf{R}^n \quad , \tag{3.77}$$

where $k > 0$ is a Lipschitz constant and $\|.\|$ is the standard Euclidean norm in $\mathbf{R}^n$. We assume that the pair $(\mathbf{C}, \mathbf{A})$ is observable. Now choose a matrix $\mathbf{K} \in \mathbf{R}^{n\times m}$ such that $\mathbf{A}_c = \mathbf{A} - \mathbf{K}\mathbf{C}$ is a stable matrix, which is always possible due to our assumption that the pair $(\mathbf{C}, \mathbf{A})$ is observable, see [36]. Then for any symmetric and positive definite matrix $\mathbf{Q} \in \mathbf{R}^{n\times n}$ there exists a symmetric and positive definite matrix $\mathbf{P} \in \mathbf{R}^{n\times n}$ such that the following well-known Lyapunov matrix equation is satisfied, see [32]

$$\mathbf{A}_c^T\mathbf{P} + \mathbf{P}\mathbf{A}_c = -\mathbf{Q} \quad . \tag{3.78}$$

For the system given by (3.76), we choose the following "observer" equation

$$\dot{\mathbf{x}}_r = \mathbf{A}\mathbf{x}_r + \mathbf{g}(\mathbf{x}_r) + \mathbf{K}\mathbf{C}(\mathbf{x} - \mathbf{x}_r) \quad , \tag{3.79}$$

which is known as the full order observer, or the Luenberger observer. Let us define the error of observation as $\mathbf{e} = \mathbf{x} - \mathbf{x}_r$. By using (3.76) and (3.79) we obtain the following error equation

$$\dot{\mathbf{e}} = (\mathbf{A} - \mathbf{K}\mathbf{C})\mathbf{e} + \mathbf{g}(\mathbf{x}) - \mathbf{g}(\mathbf{x}_r) \quad . \tag{3.80}$$

Now let the symmetric and positive definite matrices $\mathbf{P}$ and $\mathbf{Q}$ satisfy (3.78). By using the Lyapunov function $V = \mathbf{e}^T\mathbf{P}\mathbf{e}$, it can be shown that if

$$k < \frac{\lambda_{\min}(\mathbf{Q})}{2\lambda_{\max}(\mathbf{P})} \quad , \tag{3.81}$$

then we have the following

$$\|\mathbf{e}(t)\| \leq Me^{-\alpha t}\|\mathbf{e}(0)\| \quad , \tag{3.82}$$

where

$$M = \sqrt{\frac{\lambda_{\max}(\mathbf{P})}{\lambda_{\min}(\mathbf{P})}} \quad , \quad \alpha = \frac{\lambda_{\min}(\mathbf{Q})}{2\lambda_{\max}(\mathbf{P})} - k > 0 \quad ,$$

and $\lambda_{\max}(\mathbf{T})$, $\lambda_{\min}(\mathbf{T})$ denote the maximum and minimum eigenvalues of a symmetric matrix T, respectively.

In the application of the observer theory given above, the main difficulty is to satisfy the Lipschitz property given by (3.77) globally. Should (3.77) be satisfied, then the observer given by (3.79) works globally, i.e. for all $\mathbf{e}(0) \in \mathbf{R}^n$, provided that (3.81) is satisfied. This condition may be relaxed as follows, but then the result (3.82) may hold locally, i.e. in a compact region for $\mathbf{e}(0)$.

Lemma 3.4 *Consider the system given by (3.76) and (3.79). Assume that the pair* $(\mathbf{C}, \mathbf{A})$ *is observable,* $\mathbf{g} : \mathbf{R}^n \to \mathbf{R}^n$ *is differentiable and that the following is satisfied:*

$$\lim_{\mathbf{x}\to\mathbf{0}} \|D\mathbf{g}(\mathbf{x})\| = 0 \quad , \tag{3.83}$$

where $D\mathbf{g}(.)$ *denotes the Jacobian of* $\mathbf{g}$*. Then there exist a matrix* $\mathbf{K} \in \mathbf{R}^{n\times m}$ *and a real number* $r > 0$ *such that (3.82) holds if* $\|\mathbf{e}(0)\| \leq r$*, and* $\|\mathbf{x}(t)\| \leq r$*.*

Proof : See [36] and [37] □

Remark 3.4 *Note that the condition given by (3.83) is less stringent than the Lipschitz condition (3.77) and (3.81). In applications, the differential equation given by (3.76) is obtained by linearization of a nonlinear system around an equilibrium point. In such cases, the function* $\mathbf{g}$ *necessarily contains at least second order terms, consequently (3.83) is satisfied.*

The observer design technique given above assumes that an output $o(.)$ which is transmitted to the observer is available, see (3.76) and (3.79). However, in chaotic systems such an output is not given a priori, and has to be chosen as a

part of the observer design procedure. In view of the observer theory given above, obviously one should choose the output as in (3.76) so that the pair ($\mathbf{C}$, $\mathbf{A}$) is observable. We also note that for some systems, the procedure given above can be modified so that the synchronization can be acheived globally, see [36] and [37].

Chapter 4

Synchronizing Chaotic Systems: A New Approach

"The most important motive for study at school,
at the university, and in life is the pleasure of working
and thereby obtaining results which will serve the community. "
Albert Einstein

4.1 Introduction

Due to its characteristics, a chaotic system seems to be one defying any attempt of synchronization. Indeed, its high dependence on the initial conditions would magnify any small disturbance. Therefore, any two close-by trajectories rapidly diverge in phase space and quickly become uncorrelated.

Nevertheless, recent researches introduced in the previous chapter have shown the possibility to match two chaotic signals generated by two chaotic systems. Such synchronized systems usually consist of two parts: A generator of chaotic signal (drive system), and a receiver (response system).

In this chapter, we will present a synchronization scheme for chaotic systems. As in most synchronization schemes, we assume that a drive and a response system are given. The drive system generates chaotic signals among which, a few, are transmitted to the response system to be used for synchronization. In this approach we assume that a synchronizing scheme for which the synchronization is achieved exponentially fast is available, i.e., the synchronization error decays exponentially to zero. We note that this requirement is satisfied in many synchronization schemes proposed in literature , see previous chapter. The synchronization scheme proposed in this chapter conceive the following idea: The two chaotic systems aimed for synchronization will be coupled occasionally, i.e. they will be connected and then disconnected during some alternated phases, namely the synchronization and the autonomous phases. In the synchronization phases the exponential synchronization scheme mentioned above is used to synchronize the drive and the response systems and in the autonomous phases the response system is switched to an autonomous system. We show that if the synchronization and the autonomous phase intervals are chosen appropriately, then the synchronization can be achieved exponentially fast in the ideal case,(i.e. when the measurements are not corrupted with noise and parameters of the drive and response systems are exactly matched). We also show that the proposed scheme is robust to noise effect and parameters mismatch, i.e. the synchronization error remains bounded, and this bound decreases to zero as the noise and parameter mismatch magnitudes decrease to zero.

The use of occasional coupling and therefore autonomous phases is motivated by various reasons. To state a few: as mentioned in [26], in some cases it might be impossible to use only synchronization at all times. Moreover, synchronization during some finite intervals may prove to be more cost effective than steady synchronization. Another reason might be the possibility of sending chaotically masked information in the autonomous phases.

We note that a related idea for synchronization of chaotic systems was proposed in [26]. In [26], drive variables are not continuously used as an input to the response system. Instead, for a finite time step τ, at discrete instances $t = n\tau$ for $n = 0, 1, 2, \ldots$, the response system states which correspond to the drive variables used for synchronization are set to assume the values of the corresponding drive

system variables, and it was shown that for sufficiently small values of τ, the synchronization is possible. Moreover in the limit of $\tau \to 0$, this method reduces to the method of [25]. Hence in the scheme of [26], the synchronization is achieved at discrete times (i.e. not at a time interval), whereas in our scheme, which will be described later, the synchronization is achieved in an interval. We note that the length of this interval is of crucial importance for the stability analysis in our scheme. In the following sections we introduce our scheme and investigate its validity.

4.2 Occasional Coupling in Ideal Case

Assume that the drive system is given as follows:

$$\dot{u} = f(u, \mu) \quad , \quad u \in \mathbf{R}^n \quad , \quad \mu \in \mathbf{R}^p \tag{4.1}$$

where $f(.) : \mathbf{R}^n \times \mathbf{R}^p \to \mathbf{R}^n$ is a differentiable function, $\mu \in \mathbf{R}^p$ is a parameter vector. We assume that μ is such that the system (4.1) exhibits chaotic behavior. In the response system, some signals generated by (4.1) will be used for synchronization. For the sake of simplicity, let us define an "output" o generated by the system given in (4.1) as follows:

$$o = h(u) \quad , \quad u \in \mathbf{R}^n \quad , \quad o \in \mathbf{R}^m \tag{4.2}$$

where $h(.) : \mathbf{R}^n \to \mathbf{R}^m$ is a differentiable function. As a response system we consider the following differential equation:

$$\dot{w} = g(o, w, \mu) \quad , \quad w \in \mathbf{R}^n, \tag{4.3}$$

where $g(.) : \mathbf{R}^m \times \mathbf{R}^n \times \mathbf{R}^p \to \mathbf{R}^n$ is a differentiable function. Note that (4.3) signifies that the output of the drive system is used as an input to the response system for synchronization.

For the drive and the response systems described by (4.1) and (4.3), we assume that the following conditions hold:

Assumption 4.1 *The following Lipschitz condition is satisfied:*

$$\|f(u,\mu) - f(v,\mu)\| \leq k\|u - v\| \quad , \quad u, v \in \mathbf{R}^n \quad , \quad \mu \in \mathbf{R}^p \tag{4.4}$$

where $k > 0$ is a Lipschitz constant and $\|.\|$ is the standard Euclidean norm.

Assumption 4.2 *The following identity is satisfied:*

$$g(h(w), w, \mu) = f(w, \mu) \quad , \quad w \in \mathbf{R}^n \quad , \quad \mu \in \mathbf{R}^n \tag{4.5}$$

Assumption 4.3 *The drive system given by (4.1) and the response system given by (4.3) are exponentially synchronized, i.e. there exists constants $M > 0$ and $\alpha > 0$ such that for any initial time t_0 and for any initial conditions $u(t_0)$, $w(t_0) \in \mathbf{R}^n$, the following inequality is satisfied:*

$$\|u(t) - w(t)\| \leq Me^{-\alpha(t-t_0)}\|u(t_0) - w(t_0)\| \tag{4.6}$$

Remark 4.1 *The Lipschitz condition given by (4.4) might seem restrictive. However, since $f(.)$ is differentiable, (4.4) is satisfied in any compact ball, i.e. for any $r > 0$, (4.4) is satisfied for $\|u\| \leq r$ and $\|w\| \leq r$. If we assume that the drive system is chaotic, then the solutions of (4.1) which are of interest to us are bounded in a region, and consequently the assumption 4.1 is satisfied in this region. (see e.g. the postulate of Lorenz in Property 2.1),*

Assumption 4.2 is not very restrictive and is satisfied in many synchronization schemes proposed in literature, as mentioned in chapter three. As a matter of fact, the equality presented in (4.5) implies that the input to the response system is nothing but its own output fedback to itself, and hence it behaves autonomously.

Assumption 4.3 might seem restrictive. However, this condition is also satisfied in many synchronization schemes proposed in literature, e.g. Lorenz system and Chua's circuit. Recently a general synchronization scheme which guarantees exponential synchronization under some mild conditions and is applicable to a broad class of chaotic systems has been developed in [36] and [37]. □

We now state our occasional synchronization scheme, see [40]. Let the real positive numbers $T_s > 0$ and $T_a > 0$ denote the occasional synchronization and the autonomous phase interval lengths, respectively. Our scheme is summarized as follows: Letting $(i = 1, 2, \ldots)$

i : (i^{th} *occasional synchronization phase*) For $(i-1)(T_s + T_a) \leq t < iT_s + (i-1)T_a$, use the drive system given by (4.1) and the response system given by (4.3).

ii : (i^{th} *autonomous phase*) For $iT_s + (i-1)T_a \leq t < i(T_s + T_a)$, use the drive system given by (4.1) and the response system described by the following differential equation:

$$\dot{w} = g(h(w), w, \mu) = f(w, \mu) \tag{4.7}$$

Hence in our scheme occasional synchronization and autonomous phases alternate with each other. Note that with (4.7), the response system becomes an autonomous system in the autonomous phase. Since in the synchronization phase, the error decays to zero exponentially fast (assumed in (4.6)), at the end of this phase error becomes extremely small, provided that T_s is sufficiently large. Hence, in the autonomous phase we could substitute the signals of the drive system used for synchronization with the corresponding signals of the response system, which is the rationale behind using (4.7) instead of (4.3).

At this point, it might be worth noting that by making "limit" choices of T_s and T_a, our generalized scheme would resemble those described in [25] and [26]. On the one hand, if we let $T_s \to 0$ (i.e. synchronization phase interval is just an impulse), and set $T_a = \tau$, that is synchronization is performed only at some discrete times $n\tau$, $n = 0, 1, \ldots$, then our scheme reduces to that of [26]. On the other hand, if we choose $T_a = 0$ (i.e. autonomous phase does not exist), and let $T_s \to \infty$, then our scheme, presented above, reduces to that of [25]. We also note that the nonzero length of the synchronization phase $T_s > 0$ is of crucial importance for our stability analysis, see Theorem 4.1, (4.15) and (4.16) below.

For the sake of simplicity, we define T_i^s and T_i^a, the starting time of the ith

synchronization and autonomous phases respectively, as follows:

$$T_i^s = (i-1)(T_s + T_a) \quad , \quad T_i^a = iT_s + (i-1)T_a \quad , \; i = 1, 2, \ldots \tag{4.8}$$

We also define the synchronization error $e(t)$ as follows:

$$e(t) = u(t) - w(t) \tag{4.9}$$

By substituting (4.9) in (4.6), the following inequality holds in the ith occasional synchronization phase:

$$\|e(t)\| \leq Me^{-\alpha(t-T_i^s)}\|e(T_i^s)\| \quad , \quad T_i^s \leq t < T_i^a \tag{4.10}$$

From (4.1) and (4.7) it follows that the following holds in the ith autonomous phase:

$$e(t) = e(T_i^a) + \int_{T_i^a}^{t} (f(u(\tau), \mu) - f(w(\tau), \mu))d\tau \quad , \quad T_i^a \leq t < T_{i+1}^s \tag{4.11}$$

Taking norms of (4.11) results in:

$$\|e(t)\| \leq \|e(T_i^a)\| + \int_{T_i^a}^{t} \|f(u(\tau), \mu) - f(w(\tau), \mu)\|d\tau \tag{4.12}$$

Substituting (4.4) in (4.12), and using the Bellman-Gronwall lemma, see Appendix B, we obtain

$$\|e(t)\| \leq e^{k(t-T_i^a)}\|e(T_i^a)\| \quad , \quad T_i^a \leq t < T_{i+1}^s \tag{4.13}$$

Combining (4.10) and (4.13), and noting that the error is continuous at switching instances T_i^s and T_i^a we obtain:

$$\begin{aligned} \|e(t)\| &\leq e^{kT_a}\|e(T_i^a)\| \\ &\leq Me^{(kT_a - \alpha T_s)}\|e(T_i^s)\| \\ &\leq (Me^{(kT_a - \alpha T_s)})^i\|e(0)\| \quad , \quad T_i^a \leq t < T_{i+1}^s \end{aligned} \tag{4.14}$$

Now we state our first result:

Theorem 4.1 *Let the assumptions* $4.1 - 4.3$ *be satisfied and consider the occasional synchronization scheme presented above. Let the synchronization and autonomous phase intervals* T_s *and* T_a *be chosen as:*

$$T_s > \frac{\ln M}{\alpha} \tag{4.15}$$

$$T_a < \frac{\alpha T_s - \ln M}{k} \tag{4.16}$$

then for any initial $e(0)$*, the synchronization error decays to zero asymptotically, i.e.* $\lim_{t\to\infty} \|e(t)\| = 0$*. Moreover, the decay is exponential.*

Proof: From (4.14) it is obvious that if we choose T_s and T_a such that the following inequality is satisfied,

$$Me^{(kT_a - \alpha T_s)} < 1 \tag{4.17}$$

then we have $\|e(T^s_{i+1})\| < \|e(T^s_i)\|$. By using (4.17) we obtain (4.16). To guarantee that $T_a > 0$, we need to have $\alpha T_s - \ln M > 0$, and therefrom (4.15) follows. Note that (4.15) implies $Me^{-\alpha T_s} < 1$ and hence from (4.10) it follows that $\|e(T^a_i)\| < \|e(T^s_i)\|$. By using this result, (4.14) and (4.17) it follows that $\lim_{t\to\infty} \|e(t)\| = 0$.

To show that the error decays exponentially fast, note that (4.14) is valid for $T^a_i \le t < T^s_{i+1}$, which implies that $\frac{t}{T_a+T_s} < i$. Let us define $\rho = Me^{(kT_a - \alpha T_s)}$. From (4.14) we obtain

$$\|e(t)\| \le (\frac{1}{\rho})^{-i}\|e(0)\| \le e^{-\lambda t}\|e(0)\| \quad , \quad T^a_i \le t < T^s_{i+1} \tag{4.18}$$

where $\lambda = -\frac{\ln \rho}{T_a+T_s}$. Note that since $\rho < 1$, we have $\lambda > 0$, consequently (4.18) implies that the error decays exponentially to zero.□

Remark 4.2 *Theorem 4.1 does not imply that the error is continually decreasing to zero. Indeed, during the autonomous phases the error increases. However, since* $\|e(T^s_{i+1})\| < \|e(T^s_i)\|$*, it follows that the error at the end of an autonomous phase is strictly less than the error at the beginning of a preceding synchronization phase. Basically for this reason we can find an exponentially decaying function which bounds the error.*□

Remark 4.3 *In the development presented above we assume that the interval lengths T_s and T_a are invariant for all phases. However, we could vary the interval lengths in each synchronization and autonomous phase, and the result of Theorem 4.1 is still valid as far as (4.15) and (4.16) are satisfied.*□

The development presented above could be used to derive further results. For instance, assume that the initial error can be confined to satisfy $\|e(0)\| \leq r$ for some positive real $r > 0$, and it is required that the error satisfy $\|e(t)\| \leq \epsilon$ in the i^{th} autonomous phase, where $\epsilon > 0$ is a given precision level. From (4.14) it follows that this requirement can be satisfied provided that the interval lengths T_s and T_a are chosen as follows:

$$T_s > \frac{\ln M + \frac{1}{i} \ln \frac{r}{\epsilon}}{\alpha} \tag{4.19}$$

$$T_a < \frac{\alpha T_s - \ln M - \frac{1}{i} \ln \frac{r}{\epsilon}}{k} \tag{4.20}$$

Note that if we take the limit when $i \to \infty$, (4.19) and (4.20) reduce to (4.15) and (4.16). In the sequel we show the importance of (4.15) and (4.16) when we employ our scheme for the transmission of information.

4.3 Robustness with Respect to Noise and Parameter Mismatch

Consider the drive and the response system given by (4.1) and (4.3), respectively. Because of the exponential synchronization assumption, we expect that the dynamical system governing the behavior of the error (i.e. error dynamics), assumes the origin $e = 0$ as an exponentially stable equilibrium point. We note that this assumption holds in most of the synchronization schemes proposed in the literature, e.g. [18],[25],[16]. Since exponentially stable systems are robust with respect to small perturbations in the dynamics, and since our scheme is subsumed under the exponentially fast synchronizing schemes category when operating in the ideal case, we expect that the synchronization scheme suggested in the foregoing section is also robust to small perturbations.

To justify the robustness property analytically, we need to specify the error dynamics. First let us assume the ideal case, i.e. noise is suppressed and parameters match exactly. For simplicity we assume that the error dynamics is as given below:

$$\dot{e} = F(o, u, e, \mu) \tag{4.21}$$

where F is a differentiable function of its arguments, o, u and μ are as defined before. We note that the form of the error dynamics given by (4.21) is not the only possible form to conclude the robustness results. We choose this form because it could be expected from (4.1), (4.3), and also from the synchronization schemes given in [18],[25],[16]. Note that u can be considered as an exogenous signal for the error dynamics, hence we can view (4.21) as a time-varying system.

Since we assume exponential synchronization, it follows by a well-known result in Lyapunov stability theory, that there exists a Lyapunov function $V : \mathbf{R} \times \mathbf{R}^n \rightarrow \mathbf{R}$ which satisfies the following:

$$c_1\|e\|^2 \leq V(t, e) \leq c_2\|e\|^2 \tag{4.22}$$

$$\dot{V} = \frac{\partial V}{\partial t} + \frac{\partial V}{\partial e}F \leq -c_3\|e\|^2 \tag{4.23}$$

$$\|\frac{\partial V}{\partial e}\| \leq c_4\|e\| \tag{4.24}$$

for some positive constants c_1, c_2, c_3, c_4, see e.g. [41], [42]. We note that the existence of such a Lyapunov function is both necessary and sufficient for the exponential stability, see [41]. Moreover, the constants in (4.6) can be given as $M = \sqrt{\frac{c_2}{c_1}}$ and $\alpha = \frac{c_3}{2c_2}$, see [32].

In the non-ideal case, the occasional synchronization scheme presented in the previous section takes the following form:

i :(i^{th} *occasional synchronization phase*) For $T_i^s \leq t < T_i^a$, the drive system is given by (4.1) and the response system is given by the following:

$$\dot{w} = g(o + n, w, \mu') \tag{4.25}$$

where o is the output of the drive given by (4.2), n represents the noise added to the output in the transmission channel, μ' is the parameter vector of the

response system, which is slightly deviated from the parameter vector μ of the drive system. We note that the noise could be an arbitrary function of time.

ii :(i^{th} *autonomous phase*) For $T_i^a \leq t < T_{i+1}^s$, the drive system is given by (4.1) and the response system is switched to an autonomous system. Therefore in this phase, the drive system is not affected by the measurement noise and is given by:

$$\dot{w} = f(w, \mu') \tag{4.26}$$

For the robustness analysis, we need the following assumptions:

Assumption 4.4 *The following Lipschitz conditions are satisfied for some positive constants* k_1, k_2, k_3.

$$\|g(o_1, w, \mu) - g(o_2, w, \mu)\| \leq k_1 \|o_1 - o_2\| \quad , \quad o_1, o_2 \in \mathbf{R}^m, \ w \in \mathbf{R}^n, \ \mu \in \mathbf{R}^p \tag{4.27}$$

$$\|g(o, w, \mu) - g(o, w, \mu')\| \leq k_2 \|\mu - \mu'\| \quad , \quad o \in \mathbf{R}^m, \ w \in \mathbf{R}^n, \ \mu, \mu' \in \mathbf{R}^p \tag{4.28}$$

$$\|f(u, \mu) - f(u, \mu')\| \leq k_3 \|\mu - \mu'\| \quad , \quad u \in \mathbf{R}^n, \ \mu, \mu' \in \mathbf{R}^p \tag{4.29}$$

where $\|.\|$ *represents the standard Euclidean norm in* $\mathbf{R}^n, \mathbf{R}^m, \mathbf{R}^p$. □

We note that these requirement are not very restrictive. Since we assume that the signals are chaotic, and therefore bounded, (4.27)-(4.29) may be considered as a consequence of differentiability of g with respect to its arguments.

i : *Robustness in the occasional synchronization phase*

By using (4.1) and (4.3) we obtain $F(o, u, e, \mu) = f(u, \mu) - g(o, w, \mu)$ in the ideal case. Hence, by using (4.1),(4.21) and (4.25) we obtain the following error dynamics for the non-ideal case:

$$\dot{e} = F(o, u, e, \mu) + [g(o, w, \mu) - g(o, w, \mu')] + [g(o, w, \mu') - g(o + n, w, \mu')] \tag{4.30}$$

In the ideal case we have $n = 0$ and $\mu' = \mu$, and (4.30) reduces to (4.21). Since the latter is exponentially stable, the terms in square brackets in (4.30) represent

perturbations to an exponentially stable system. By using the exponential stability of the error dynamics in the ideal case, we can prove the following result for (4.30).

Theorem 4.2 *Consider the error dynamics given by (4.30). Assume that (4.27) and (4.28) hold. Let the noise n satisfy* $\|n(t)\| \leq n_m$ *for some positive real number* $n_m > 0$ *for* $t \geq 0$ *and let us define* $\Delta\mu = \mu - \mu'$. *Then the error asymptotically (i.e. as* $t \to \infty$*) satisfies the following inequality:*

$$\|e(t)\| \leq C_1 n_m + C_2 \|\Delta\mu\| \tag{4.31}$$

where $C_1 > 0$ *and* $C_2 > 0$ *are some constants.*

Proof: Let us consider the Lyapunov function which satisfies (4.22)-(4.24). Since the error dynamics is exponentially stable in the ideal case, such a function always exists. By differentiating V along the solutions of (4.30), we obtain:

$$\begin{aligned} \dot{V} &= \frac{\partial V}{\partial t} + \frac{\partial V}{\partial e} F + \frac{\partial V}{\partial e} [g(o, w, \mu) - g(o, w, \mu')] \\ &\quad + \frac{\partial V}{\partial e} [g(o, w, \mu') - g(o + n, w, \mu')] \\ &\leq -c_3 \|e\| (\|e\| - \frac{c_4}{c_3}(k_1 n_m + k_2 \|\Delta\mu\|)) \end{aligned} \tag{4.32}$$

where we used (4.23),(4.24),(4.27) and (4.28). From (4.32) it follows that if $\|e\| > \frac{c_4}{c_3}(k_1 n_m + k_2 \|\Delta\mu\|)$, then $\dot{V} < 0$, consequently, error e "decreases" along the solutions of (4.30). It then follows from the standard invariance arguments that (4.31) is asymptotically satisfied, see Appendix C. In particular we could choose $C_1 > \frac{c_4}{c_3} k_1$ and $C_2 > \frac{c_4}{c_3} k_2$, where c_3 and c_4 are given by (4.23) and (4.24), respectively. □

It follows from (4.31) that if n_m and $\|\Delta\mu\|$ are sufficiently small, then the error will be asymptotically small. Hence, we can conclude that synchronization schemes for which error dynamics is exponentially stable, is also robust with respect to noise and parameter mismatch. We note that this result is the basic reason for the robustness of many schemes proposed for synchronization in literature. Hence, we can view Theorem 4.2 not only as a result related to the

synchronization scheme proposed here, but also as a general result related to any synchronization scheme, provided that its assumptions are satisfied. We also note that the above result is only asymptotical in nature and the required synchronization length T_s can not be specified in general. To estimate the required T_s, further assumptions on the form of the error dynamics given by (4.21) may be necessary, see [37] [36].

ii : Robustness in the autonomous phase

By using (4.1) and (4.26), we obtain the following in the autonomous phase:

$$\begin{aligned} e(t) &= e(T_s) + \int_{T_s}^{t} [f(u(\tau),\mu) - f(w(\tau),\mu)]\, d\tau \\ &\quad + \int_{T_s}^{t} [f(w(\tau),\mu) - f(w(\tau),\mu')]\, d\tau \quad , \quad t \geq T_s \end{aligned} \tag{4.33}$$

Taking norms of (4.33) and using (4.4) and (4.29), we obtain:

$$\|e(t)\| \leq \|e(T_s)\| + k_3\|\Delta\mu\|(t - T_s) + \int_{T_s}^{t} k\|e(\tau)\| d\tau \quad , \quad t \geq T_s$$

Now assume that the autonomous phase takes place in the interval $T_s \leq t < T_s + T_a$. Then, by using Bellman-Gronwall inequality we obtain:

$$\|e(t)\| \leq (\|e(T_s)\| + k_3\|\Delta\mu\|T_a)e^{kT_a} \quad , \quad T_s \leq t < T_s + T_a \tag{4.34}$$

Now assume that $\|e(T_s)\| \leq \epsilon_s$ and we require $\|e(t)\| \leq \epsilon_a$ for $T_s \leq t < T_s + T_a$ for some precision levels $\epsilon_s > 0$, $\epsilon_a > 0$. Obviously we should have $\epsilon_a > \epsilon_s$. Then from (4.34) it follows that T_a should satisfy:

$$e^{kT_a} < \frac{\epsilon_a}{\epsilon_s + k_3\|\Delta\mu\|T_a} \tag{4.35}$$

Actually, there exists a $T > 0$ such that (4.35) is satisfied for all $0 \leq T_a \leq T$. To see that, note that (4.35) is satisfied for $T_a = 0$. Since the left and right sides of (4.35) are strictly increasing and decreasing functions of T_a, respectively, it follows that such a $T > 0$ exists.

Note that in the ideal case we have $\Delta\mu = 0$ and $\epsilon_s = Me^{-\alpha T_s}r$ where $\|e(0)\| \leq r$, see (4.35). If T_s satisfies (4.15), then $Me^{-\alpha T_s} < 1$, hence we can choose $\epsilon_a = r$. With this choice, (4.35) reduces to (4.16) in the ideal case.

From the analysis presented above it is clear that if we choose T_s sufficiently large and apply our occasional synchronization scheme, it is possible to keep the error below a reasonable precision level. From a practical point of view, T_s and T_a should be chosen sufficiently larger and smaller than the bounds given by (4.15) and (4.16), respectively.

4.4 Application to Information Transmission

The main application of synchronization of chaotic systems that has been proposed so far is to hide an information carrying signal in a chaotic carrier signal. This can be viewed as analog cryptography. The master system is the transmitter and the slave system being the receiver. The cryptographic key is the parameter set of the chaotic system, namely the parameter vector μ. In this section, we present a chaotic masking scheme and recovery scheme using the synchronizing approach introduced in the preceding section. In this method, the synchronization and the message sending phases are separated. During the synchronization phase, the transmitter synchronizes the receiver, thereafter, in the autonomous phase an information bearing signal $m(t)$ is added to the output $o = h(u)$ of the transmitter chaotic signal and then sent to the receiver. The latter keeping on synchronized with the transmitter during the autonomous phase, as already shown, produces $h(w) \approx h(u)$ and hence by simple subtraction the information carrying signal may be recovered. Next we show how message transmission may be performed in ideal conditions as well as in real conditions.

4.4.1 Transmission in Ideal Case

Consider the transmitter and the receiver systems defined by (4.1) and (4.3) respectively. Assume that (4.4)-(4.6) are satisfied, additionally we assume the following is satisfied

$$\|h(u) - h(w)\| \leq c\|u - w\| \quad , \quad u, w \in \mathbf{R}^m \tag{4.36}$$

for some $c > 0$. The assumption given in (4.36) seems stringent, however since $h(.)$ is differentiable, the arguments stated in Remark 4.1 are also available to justify (4.36).

We now state our message transmission method, see [43]. Let $m(t)$ be the information bearing signal. Let $T_s > 0$ and $T_m > 0$ denote the interval lengths of the synchronization and message transmission phases, respectively. (Here, T_m and "message transmission" terms substituted T_a and "autonomous" terms.) Our scheme is described below:

i : (*Synchronization phase*) For $0 \leq t < T_s$, send the synchronization signal o to the response system given by

$$\dot{w} = g(o, w, \mu)$$

ii : (*Message transmission phase*) For $T_s \leq t < T_s + T_m$, send the masked message $o(t) + m(t)$, to the response system given by

$$\dot{w} = g(h(w), w, \mu) = f(w, \mu)$$

iii : (*Message recovery*) For $T_s \leq t < T_s + T_m$, the information bearing signal may be recovered through this operation

$$m_r(t) = o(t) + m(t) - h(w(t)) \tag{4.37}$$

Note that the information carrying signal is sent during the autonomous phase during which the error increases and may taint the information, and hence the synchronization interval length T_s should be determined accordingly. For this purpose we developed the following result

Theorem 4.3 *Consider the systems given by (4.1), (4.3) in the synchronization phase and (4.1), (4.7) in the message transmission phase. Assume that Assumptions 4.1 and 4.3 hold and consider the message transmission-recovery scheme given above. Let the initial error satisfy* $\|u(0) - w(0)\| \leq r$ *for some* $r > 0$*, and let (the precision number)* $\epsilon > 0$ *be given. Then, for any* $T_m > 0$ *and for any message of length* T_m*, there exists a synchronization interval length* $T_s > 0$ *such that in the message transmission phase we have*

$$\|m_r(t) - m(t)\| \leq \epsilon \quad , \quad T_s \leq t < T_s + T_m \tag{4.38}$$

Note that $m_r(t)$ stands for the recovered signal.

Proof: Similar to the derivations preceding Theorem 4.1, we take norms of (4.38) and using (4.1) and (4.7), in addition to Bellman-Gronwall lemma, we obtain

$$\|u(t) - w(t)\| \leq e^{k(t-T_s)}\|u(T_s) - w(T_s)\| \quad , \quad t \geq T_s \tag{4.39}$$

Substituting (4.6) in (4.39) we obtain

$$\|u(t) - w(t)\| \leq Me^{kt}e^{-(k+\alpha)T_s}\|u(0) - w(0)\| \quad , \quad t \geq T_s \tag{4.40}$$

The right hand side of (4.40) is maximum at the end of the message sending interval, (i.e. at $t = T_s + T_m$), hence for $T_s \leq t < T_s + T_m$ we have

$$\|m_r(t) - m(t)\| = \|h(u(t)) - h(w(t))\| \leq cMe^{(kT_m - \alpha T_s)}\|u(0) - w(0)\| \tag{4.41}$$

where we used (4.2),(4.36),(4.37) and (4.40). It follows from (4.41) that by choosing appropriate T_s and T_m we could successfully send and recover information. Eventually, we may easily show using (4.41) that the synchronization interval length T_s should satisfy

$$T_s > \frac{kT_m + \ln \frac{cMr}{\epsilon}}{\alpha} \quad \square \tag{4.42}$$

Remark 4.4 *The precision number could be defined in several ways, an alternative definition is to choose* $\epsilon > 0$ *as the maximum magnitude of noise that if added to a message it does not spoil it. (i.e. if the message is sound then it retains its audibility with acceptable quality.)*

Remark 4.5 *The expression of (4.40) states that the above theorem is proved for the first synchronization and message transmission phases. Actually, the result is available for any i^{th} phases, by performing time shift and considering the error at the end of the $(i-1)^{th}$ message transmission phase as the initial error of the i^{th} synchronization phase, and T_m to be the length of the i^{th} piece of information to be transmitted.*

4.4.2 Transmission in Real Case

For the real case, the transmission of information will be irritated by the presence of noise in addition to parameter mismatch. Therefore, we consider the transmitter and receiver systems defined by (4.1) and (4.25) , for the synchronization phase, and the systems defined by (4.1) and (4.26) for the message transmission phase. For the synchronization phase results have been developed in the former section, whereas for the message transmission phase we present the following results

Theorem 4.4 *Consider the system given by (4.1) and (4.26) and the message transmission scheme given in the previous subsection. Assume that the synchronization interval is sufficiently long so that (4.31) is satisfied. Let $\epsilon > 0$ be a given precision number. If*

$$\frac{cc_4}{c_3}(k_1 n_m + k_2\|\Delta\mu\|) < \epsilon \tag{4.43}$$

where the constants used here are as given in Assumption 4.4 and equations (4.36)(4.23)(4.24), then there exists a maximum allowable message transmission interval $T > 0$ such that if $T_m \leq T$, then in the message transmission interval the following holds:

$$\|m_r(t) - m(t)\| \leq \epsilon \quad , \quad T_s \leq t < T_s + T_m \tag{4.44}$$

Proof: Let us define $A = \frac{cc_4}{c_3}(k_1 n_m + k_2\|\Delta\mu\|)$ and $B = k_3\|\Delta\mu\|$. Then, from (4.34) and (4.36) it follows that such T exists if the following inequality is

satisfied:

$$e^{kT_m} \leq \frac{\epsilon}{A + BT_m} \tag{4.45}$$

From (4.43) it follows that (4.45) is satisfied when $T_m = 0$. The left and right hand sides of (4.45) are strictly increasing and strictly decreasing functions of T_m, respectively. Hence it follows easily that a $T > 0$ exists. □

Intuitively we note that the error decay, albeit exponential, can not go beyond some level created by the presence of noise and parameters mismatch, and any larger initial error may be further decreased to that specific level. Therefore, based on (4.31) and (4.37) assumption (4.43) is natural. We also note that (4.31) gives an upper bound for the error when the synchronization interval is long enough, meanwhile it defines a lower bound on the message magnitude level, beyond which the message may be confused with error. In most of the message transmission schemes proposed in literature, the message magnitude level should be significantly small compared to the chaotic signal, and hence can be menaced by error distortion, see [20]. We emphasize that in the ideal case, the magnitude level of the message is not limited in our scheme, and in the non-ideal case this level should be sufficiently higher than the error bounds given by (4.31). This flexibility of the message level (i.e. absence of upper bound) may be considered as an advantage.

From (4.45) it follows easily that the maximum allowable transmission length T depends on n_m and $\|\Delta\mu\|$ continuously and that T becomes larger as n_m or $\|\Delta\mu\|$ become smaller. In the limit when $n_m = 0$ and $\Delta\mu = 0$ (ideal case), we have $T = \infty$ and for any T_m we can have successful message recovery, provided that T_s is sufficiently long. In the non-ideal case, we have $T < \infty$, and the length of T_m does not depend on T_s but solely on the noise level and parameter mismatch as (4.45) implies. Therefore, if the message to be transmitted is larger than the maximum allowable transmission length $T_m > T$, then the message should be divided into shorter pieces, each of which is less than T. This point may be considered as a disadvantage of our scheme.

Chapter 5

Simulation and Experiment Results

"Perfect logic and faultless deduction make a pleasant theoretical structure, but it may be right or wrong The experimenter is the only one to decide, and he is always right. "

L.Brillouin

To validate the new method proposed in the previous chapter, for the synchronization of chaotic systems, we performed numerical (MATLAB) as well as electronic (H-SPICE) simulations. Having obtained promising results, we, afterwards, performed some laboratory experiments. The results of this work are summed up in this chapter.

5.1 Numerical Simulation

Numerical simulations were carried out using MATLAB and specifically the SIMULINK package, it is merely an analysis of the system governing equations. To start with, we consider the scaled Lorenz system, presented in chapter two,

as the drive system

$$\begin{aligned} \dot{x} &= \sigma(y - x) \quad , \\ \dot{y} &= -20xz + rx - y \quad , \\ \dot{z} &= 5xy - bz \quad . \end{aligned} \tag{5.1}$$

We choose the parameters σ, r and b so that the system (5.1) is in the chaotic regime as $\sigma = 10$, $r = 20$, $b = 1$. We note that (5.1) is in the form (4.1). The solution $x(t)$ of (5.1) will be used to synchronize the solutions of the following response system

$$\begin{aligned} \dot{x}_r &= \sigma(y_r - x_r) \quad , \\ \dot{y}_r &= -20xz_r + rx - y_r \quad , \\ \dot{z}_r &= 5xy_r - bz_r \quad . \end{aligned} \tag{5.2}$$

In our notations we have $o = x$, hence $m = 1$, and with $u = (x\ y\ z\ )^T$, we have $o = h(u) = Cu$ with $C = (1\ 0\ 0)$. Also note that the response system is of the form given by (4.3), moreover (4.4) and (4.5) are satisfied.

In order to apply our scheme, we should prove that systems (5.1) and (5.2) synchronize exponentially fast. Indeed, this was proved in chapter three. Furthermore, we can show that the error system is globally asymptotically stable if we use the following Lyapunov equation

$$V(t, e) = \frac{1}{\sigma} e_x^2 + e_y^2 + 4e_z^2$$

thus

$$\dot{V}(t, e) = -2e_x^2 + 2e_x e_y - 2e_y^2 - 8be_z^2$$

using the fact $2pq \leq p^2 + q^2$ we get

$$\dot{V}(t, e) \leq -e_x^2 - e_y^2 - 8be_z^2$$

since $b = 1$

$$\dot{V}(t, e) \leq -\|e\|^2$$

using TheoremA.2 we conclude that the error system is globally asymptotically stable. Moreover from Theorem A.3 that the error system is exponentially stable, consequently synchronization is exponentially fast.

Now since the function f given by (4.1) and (5.2) is differentiable, it follows that (4.4) is satisfied in any compact region in state space. In particular, we have $k \leq \sup\{\|\frac{\partial f}{\partial u}\| \mid \|u\| \leq r\}$ for any $r > 0$.

We start by estimating the bounds given by (4.15) and (4.16). By using the previous derivations, we notice that (4.22)-(4.24) are satisfied with $c_1 = 0.1$, $c_2 = 4$, $c_3 = 1$, and hence (4.6) is satisfied with $M = 6.32$ and $\alpha = 0.125$. Also by simulating (5.2), we estimated the Lipschitz constant in (4.4) as $k = 18.64$, see [40]. Applying these constants to the inequality in (4.15) we found that $T_s \geq 14.75$ *sec.* is required, and if we choose $T_s = 15$ *sec.*, the inequality in (4.16) requires $T_a \leq 0.02$ *sec.* However, in our simulations we were able to obtain longer autonomous phase intervals. This shows that the estimates given in (4.15) and (4.16) are quite conservative.

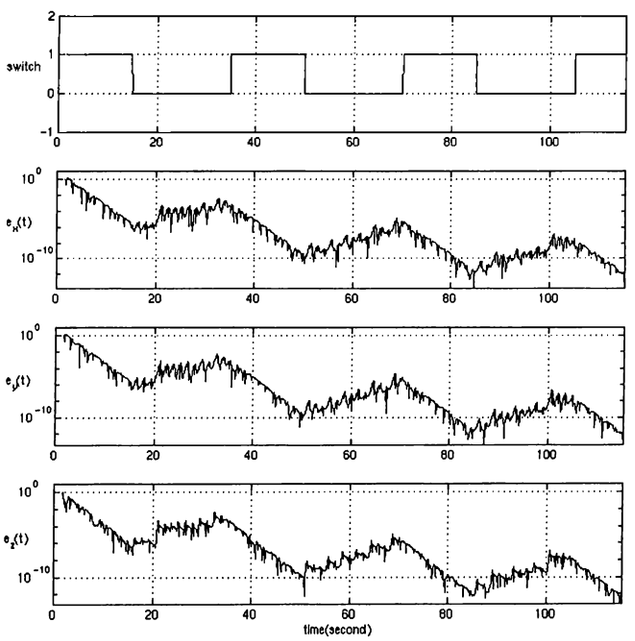

Figure 5.1: Synchronization of Lorenz system by using occasional coupling.(ideal case

In the first set of simulations, we considered the ideal case and choose $T_s = 15$ *sec.* and $T_a = 20$ *sec.* Since the origin is an equilibrium point of Lorenz system,

we assigned the initial conditions $x(0) = 0.8$, $y(0) = 0.1$, $z(0) = 2$ for the drive system to commence the chaotic oscillations. For the response system, however, we chose zero initial conditions. The results of the simulation are depicted in Figure 5.1 . The uppermost graph shows the synchronization and autonomous phase intervals delineated by the switch values 1 and 0 respectively. The other graphs show the evolution of the errors e_x, e_y and e_z, respectively. We note that the errors are decreasing exponentially (linearly on the logarithmic scale.) during the synchronization phases and increase during the autonomous phases, besides, two successive synchronization phases start with different initial errors, with the first one having a larger error. It is worth noting that in the autonomous phase the divergence is also exponential, and since divergence is governed by the Lyapunov exponent, we prefer to use systems with lower Lyapunov exponents.

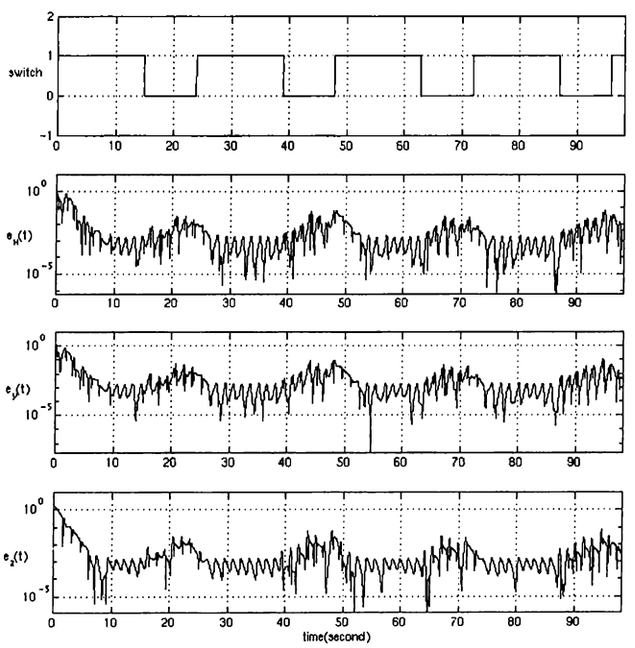

Figure 5.2: Synchronization of Lorenz system by using occasional coupling.(real case)

In the second set of simulations we consider the non-ideal case and choose $T_s = 15$ *sec.* and $T_a = 10$ *sec.* We have again used the same initial conditions for

both the drive and the response systems. The parameters of the response system are $\sigma' = 10.01$, $r' = 20.02$, $b' = 1.001$, which corresponds to a mismatch of 0.1%. We also added a white noise generated by the computer, to the synchronizing signal; the magnitude of the white noise is bounded by $n_m = 10^{-4}$. The results of the simulation are shown in Figure 5.2. It can be seen from the figures that the errors remain bounded, and its bound is comparable to the noise level.

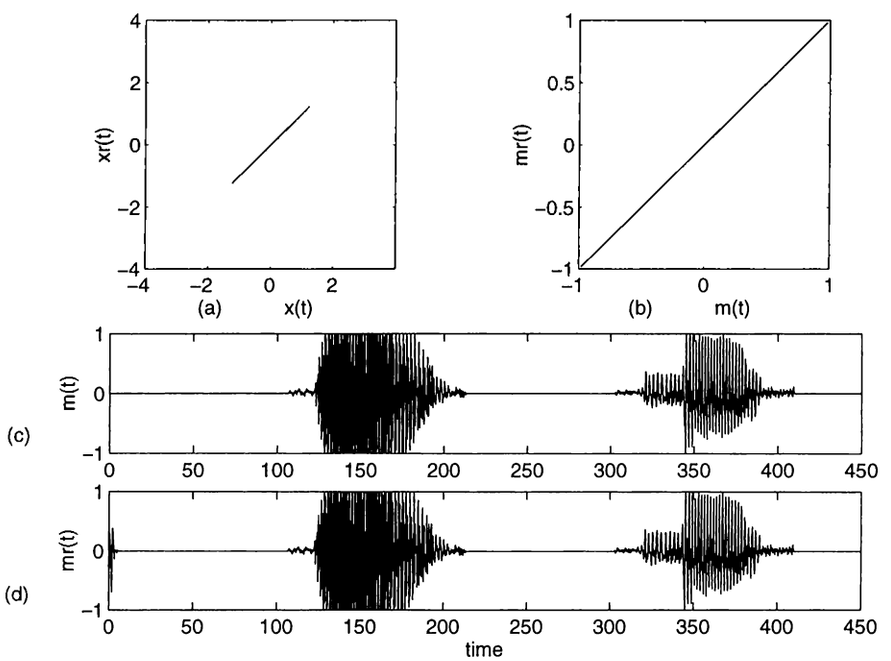

Figure 5.3: Transmission of information using chaotic carrier.(Ideal case)

The application of information transmission to Lorenz system was also successful. First the method may be summarized as follows, let $T_m > 0$ be given and $T_s > 0$ appropriately chosen then we have

i : (*Synchronization phase*) For $0 \leq t < T_s$, send the synchronization signal $x(t)$ to the response system given by (5.1)

ii : (*Message transmission phase*) For $T_s \leq t < T_s + T_m$, send the masked message $x(t) + m(t)$, to the response system given by

$$\dot{x}_r = \sigma(y_r - x_r) \quad ,$$

$$\dot{y}_r = -20x_r z_r + rx_r - y_r \quad , \tag{5.3}$$
$$\dot{z}_r = 5x_r y_r - bz_r \quad .$$

iii : (*Message recovery*) For $T_s \leq t < T_s + T_m$, the recovered message $m_r(t)$ is;

$$m_r(t) = x(t) + m(t) - x_r(t)$$

Figure 5.3 depicts an example of information transmission. In this case the chaotic systems used for transmission are ideal. A speech signal corresponding to the sounds of the letters "A" and "B", was masked, sent and then recovered successfully with good audible quality. The speech signal was created using the sound tools of Sun Sparcstations, with a sampling frequency of 8 kHz. Note that the message level is comparable to the chaotic signal level, thus confirming that our scheme is free from any upper bound restrictions.

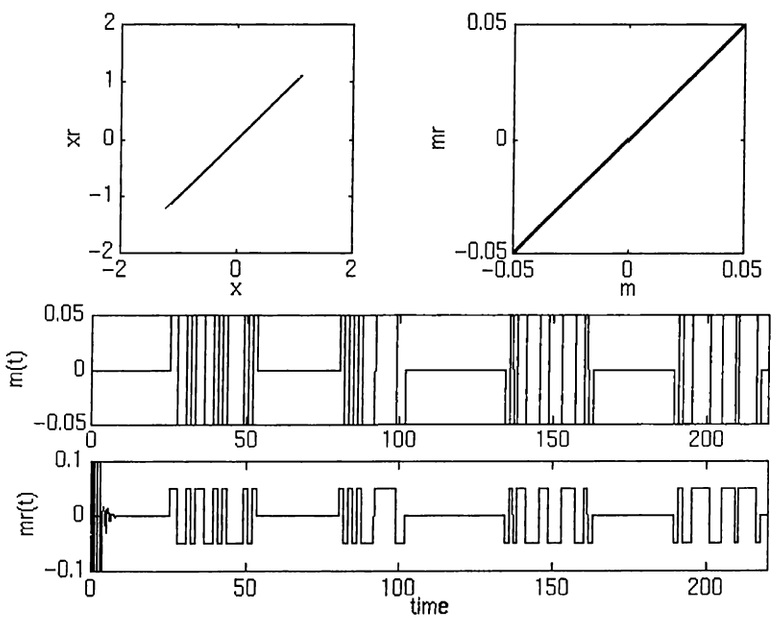

Figure 5.4: Transmission of information using chaotic carrier.(Real case)

Figure 5.4 depicts another example of information transmission. In this case a white noise bounded by $n_m = 10^{-4}$ was added to the transmitted signal. The

parameters of the response system were mismatched by a percentage of 0.1%, i.e. $\sigma' = 10.01$, $r' = 20.02$, $b' = 1.001$. The resulting systems were used to transmit and recover the sentence "wish you good luck" coded by using the standard international alphabet code no 2. Since in this case we deal with a long message, we divided the message into four parts, and sent each word in one message transmission interval, we also note that the message level is very low compared to the chaotic signal but high enough not to be corrupted with noise, the results showed that the message was successfully recovered.

In the next two simulations we tried to see the effect of the noise and parameter mismatch on the message transmission length T_m. First we assumed that only noise is present and parameters of drive and response systems are perfectly matched.

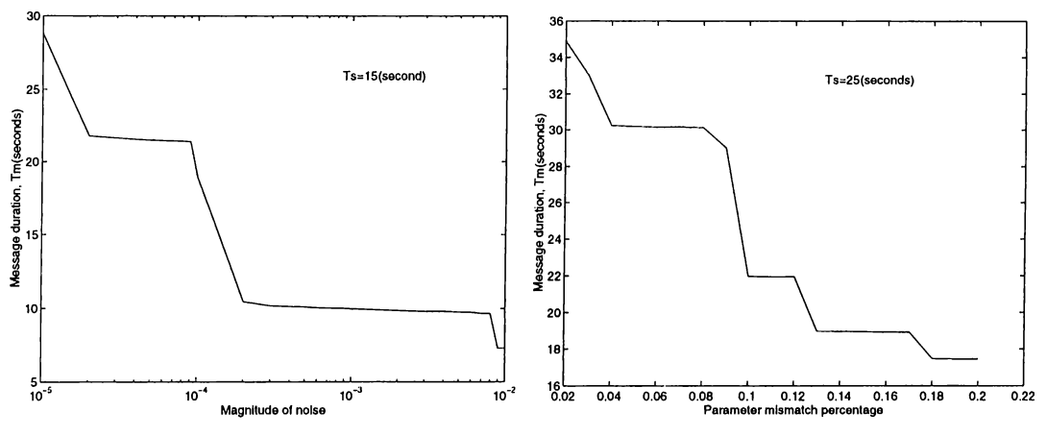

Figure 5.5: Noise and parameter mismatch effects on the length of transmitted message.

We considered a sine wave with fixed amplitude and frequency as the message to be transmitted, and used $T_s = 15$ *sec.* as synchronization interval length, we let the precision level to be less than 5% of the message level. The simulation was performed for various noise amplitudes, ranging from 10^{-5} to 10^{-2}, on a logarithmic scale. The results are shown in Figure 5.5. As can be seen, T_m decreases with increasing noise level, which is expected. Next, we assumed that the system is noise-free but systems parameters are p % mismatched. Here p % mismatch means that all the parameters of the response system are $1 + 0.01p$ larger than those of the drive system. We performed this simulation for various

values of p ranging over $[0.02, 0.2]$. The results shown in Figure 5.5 confirm the expectations: T_m decreases with increasing p.

5.2 Electronic Simulation and Experiment

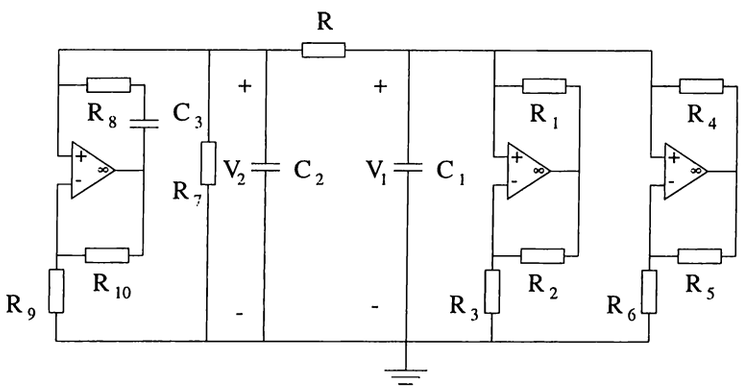

Figure 5.6: Wien bridge based chaos generator.

As a fore-step of laboratory work, H-spice simulations were carried out to have closer idea on realistic results. The first step was to continue on simulating the Lorenz system represented by the circuit introduced in chapter two. However, we encountered several difficulties, namely: multipliers needed to be modeled using the nonlinear voltage controlled voltage source, and no existing H-spice macro-model fulfilled the task. Besides, the simulation of only one Lorenz system required long time as well as extremely large memory, which discouraged us from going on simulating the whole communication system containing a drive and response Lorenz systems in addition to the switch, adder and subtracter. Due to the foregoing reasons, we prefered to use Chua's circuit to substantiate the theory we have presented about our synchronization scheme. Since the circuit to be simulated represents a basis for the experimental work, we thought about the difficulties that we might encounter if we desire to implement Chua's circuit, indeed a high valued inductor may represent an obstacle towards our aim. Actually, most of the chaotic signal generators proposed in literature contain inductors, which is inconvenient for various reasons. For example, inductors are less standard if compared to other circuit elements and have to be prepared separately in most

applications. They are not as ideal as other circuit elements, and in terms of spatial dimensions they are bigger in size than the other circuit elements, unless the inductance is rather small. The circuits which contain capacitors instead of inductors are more convenient in this sense. To accomplish our aim (performing simulation with a practical circuit), we used the circuit suggested in [9] which is described below and depicted in Figure 5.6.

We note that Chua's circuit contains two mere parts, namely: The nonlinear resistor (Chua diode) and a harmonic oscillator which contains a capacitor and an inductor. The idea described in [9] is based on substituting the LC harmonic oscillator by a device which does not contain inductors, meanwhile sustaining oscillations, for this purpose the Wien bridge oscillator was suggested. Figure 5.7 shows the chaotic behavior of the circuit shown in Figure 5.6, and with the component values stated in Table 5.1.

Components	Values/code
Op-amps	Texas Instruments lf351
R	$1k\Omega$ in series with $1k\Omega$ CITEC CT 10 V
R_1	$22k\Omega$
R_2	$22k\Omega$
R_3	$3.3k\Omega$
R_4	220Ω
R_5	220Ω
R_6	$2.2k\Omega$
R_7	100Ω
R_8	100Ω
R_9	100Ω
R_{10}	470Ω CITEC CT 10 H
C_1	$15nF$
C_2	$2.2\mu F$
C_3	$2.2\mu F$

Table 5.1: Component types and values of the experimented circuit.

Similar to Chua's circuit, the synchronization of the Wien bridge based chaos

generator may be proved, indeed, the synchronization has been shown via simulation and experiment.

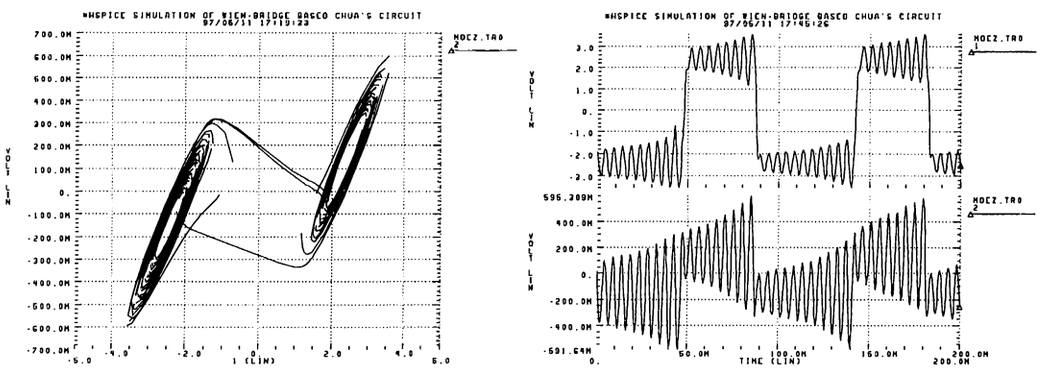

Figure 5.7: Dynamic behavior of the Wien bridge based chaos generator.(Results obtained via H-spice simulation)

Now we consider the overall synchronizing and transmitting system described by the block diagram shown in Figure 5.8. The master chaotic system is the Wien bridge based circuit, where $V_{C1}(t)$ was used to synchronize and mask the information signal in the synchronization and message transmission intervals respectively. Buffers have been used not to doom the chaotic behavior of the circuit, since the input resistance of the switch and the adder is not high enough and may render the chaotic system a stable one. We also note that two inverse sign adders were used instead of an adder and a subtracter in order to optimize the size of the overall system, and the recovering equation becomes:

$$\begin{aligned} m_r(t) &= -(V_{C1}^r(t) - (V_{C1}(t) + m(t))) \\ &= V_{C1}(t) + m(t) - V_{C1}^r(t) \end{aligned}$$

Another step to optimization was the use of the ADG413 switch from Analog-Devices production containing four switches, two of them are logically inverted compared to the others, hence providing "S" and "$\bar{\text{S}}$" switches in a single chip. The filter, however, should be determined according to the type of the sent message e.g. for the case of binary messages we used a comparator.

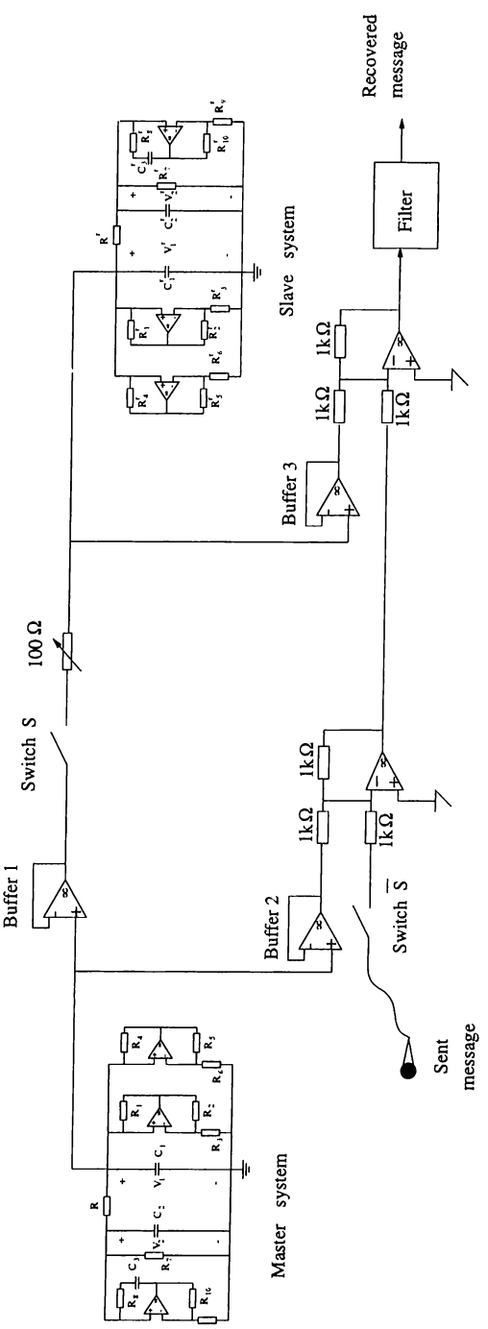

Figure 5.8: Block diagram of the synchronization and transmission system.

The simulation results are depicted in Figure 5.9. The upper most graph shows the switch controlling voltage which drives the switch "ON" if the voltage is high (12V) and "OFF" if the voltage is low (0V). Next two graphs show the error between the drive and response signals, namely: $v_{C1} - v_{C1}^r$ and $v_{C2} - v_{C2}^r$. The sent message is shown in the fourth graph, the fifth and sixth graph show the recovered message before and after filtering respectively. We note that $T_s = 24\ msec.$ and $T_a = 36\ msec.$ and the message recovery was successfully achieved.

Having obtained promising results, we afterwards started the experimental work. We first started by experimenting the Wien bridge chaos generator having the same component values found in [9]. This experiment was confronted by various difficulties such as high tolerances (e.g. 5% *to* 10%) of the standard resistors and capacitors. As a result the synchronization error was significantly high (e.g. 10% − 12% of the synchronizing signal level). Besides, the chaotic oscillations were high and depending on the frequency of the Wien bridge oscillator ($f_0 = 33.8kHz$), hence it was difficult for the slave system to track the behavior of the master system. As a remedy for these difficulties, we had to, pair-wisely, select components having closest values and we had to reduce the oscillating frequency of the Wien bridge oscillator while maintaining the system in the chaotic regime. Next, we have reduced the frequency of the oscillator to $f_0 = 7.3kHz$ then to $f_0 = 3.4kHz$, the experiments carried out at these frequencies showed better performances with a synchronizing error of 7% *to* 10%. Eventually, we have reduced the frequency to $f_0 = 728Hz$, and we implemented the chaos generator shown in Figure 5.6 with the component values given in Table 5.1.

We note that the experiment was carried out using a DC generator Hewlett Packard 6628A, a function generator MODEL: GFG-8019G. The outputs were obtained using the oscilloscope Hewlett Packard 54600B and plotter Hewlett Packard 7475A.

Due to imperfections of the experiment, we expected a regression in the results compared to the simulations. Indeed the presence of a significant noise level and parameter mismatch in our system reduced the ratio of the autonomous interval length T_a to the synchronization interval length T_s. While in the simulations $T_s = 24msec.$ and $T_a = 36msec.$, from the experiment we could at best obtain

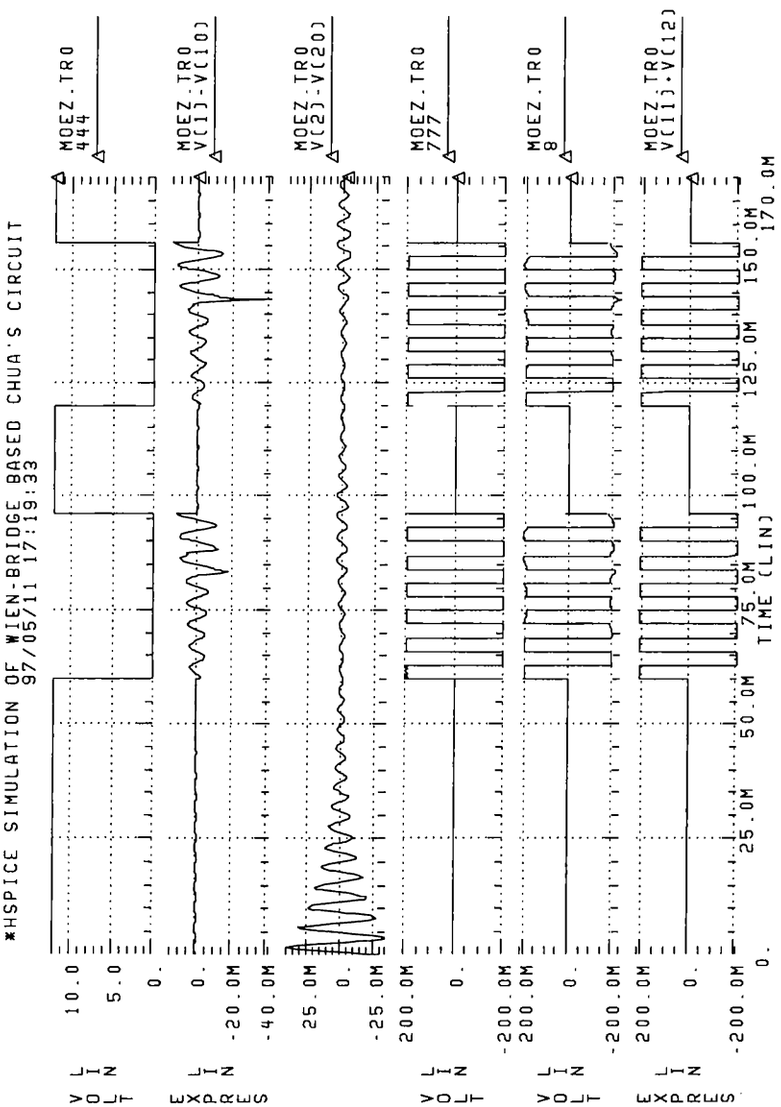

Figure 5.9: Information transmission using chaotic masking.(H-spice simulation)

an autonomous interval length of $T_a = 1.84msec.$ for a synchronization interval length $T_s = 9.63msec.$. We note that since the error is lower bounded by the noise level, a longer synchronization phase e.g. $T_s = 16msec.$ results in the "same" autonomous phase $T_a = 1.87msec.$, the slight difference may be due to reading error. Figure 5.10 depicts the switch signal which leaded to the highest T_a/T_s ratio we could obtain.

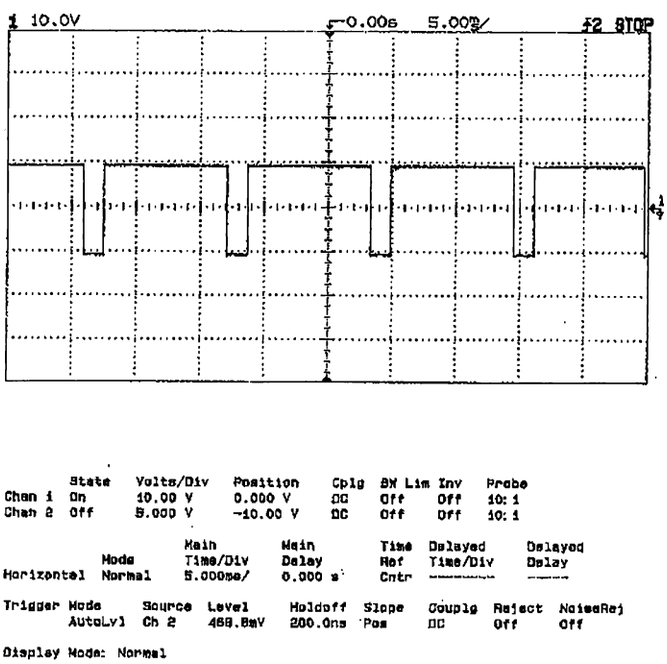

Figure 5.10: The switch signal that governs T_s and T_a. (Experiment results)

To show that the system is operating in the chaotic regime, we have obtained the double scroll shown in Figure 5.11. We note that the depicted double scroll is not a limit cycle. Actually, Figure 5.11 also shows the drive signal in addition to its power spectrum density. The data describing the time evolution of the drive signal was obtained by using the HP-IB input deck shown in Appendix D. We note that the drive signal was sampled with a sampling period of $0.02msec.$, during an interval of $50msec.$ Then by using MATLAB we have plotted the time evolution as well as the power spectrum density of the drive signal(on a normalized frequency scale). The latter shows that the signal is broadband and hence the double scroll in Figure 5.11 is not a limit cycle. We note that the

drive signal plotted using MATLAB is not sufficiently smooth despite the high sampling frequency, this is due to inaccurate readings from the oscilloscope.

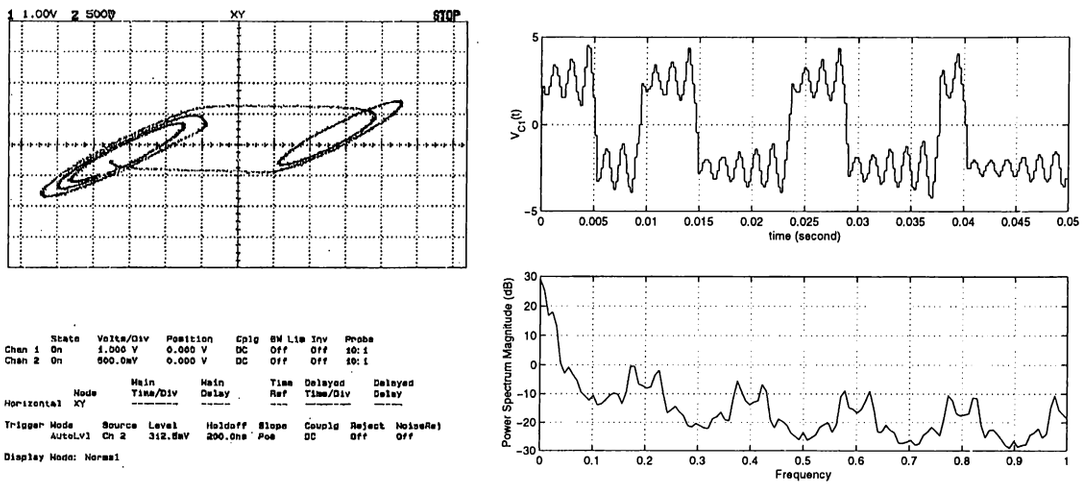

Figure 5.11: Double scroll $V_{C1} vs V_{C2}$ and The drive signal time evolution and its power spectrum density

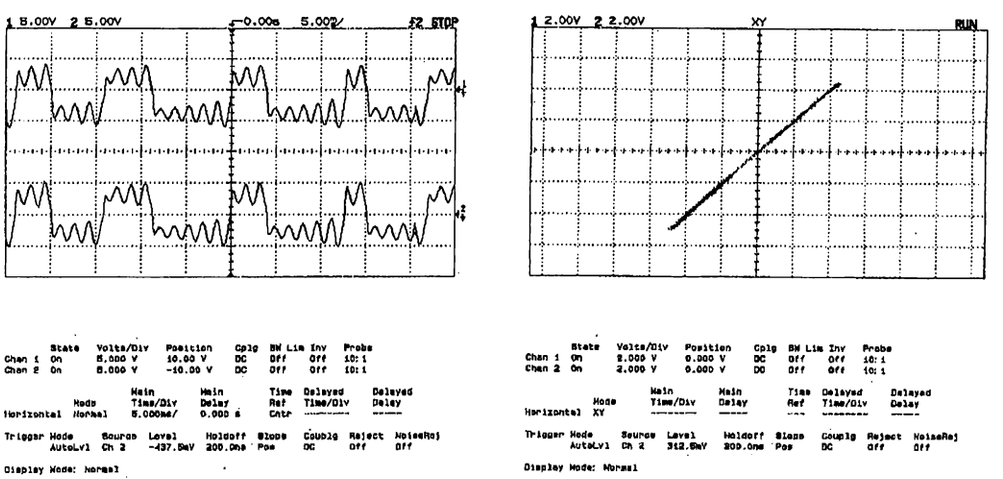

Figure 5.12: Drive and response signals, $V_{C1}(t)$ and $V_{C1}^r(t)$ and V_{C1} *vs* V_{C1}^r

Figure 5.12 shows two graphs. The first one depicts the drive signal and the response signal time evolution. We may easily note that they are identical for all times, hence the system is kept synchronized during the autonomous phases. The second graph shows V_{C1} versus V_{C1}^r, which is a clear 45^o line confirming that

the signals are identical. In fact, a small error exists due to noise and parameter mismatch. This error was measured by subtracting the response from the drive signal and obtained to represent 3% of the signal level (i.e. $260mV peak\ to\ peak$).

Figure 5.13 shows signals $V_{C2}(t)$ and $V_{C2}^r(t)$ besides V_{C2} *vs* V_{C2}^r. Again the signals are synchronized at all times and a small error was measured to represent 4% of the signal level (i.e. $25mV peak\ to\ peak$).

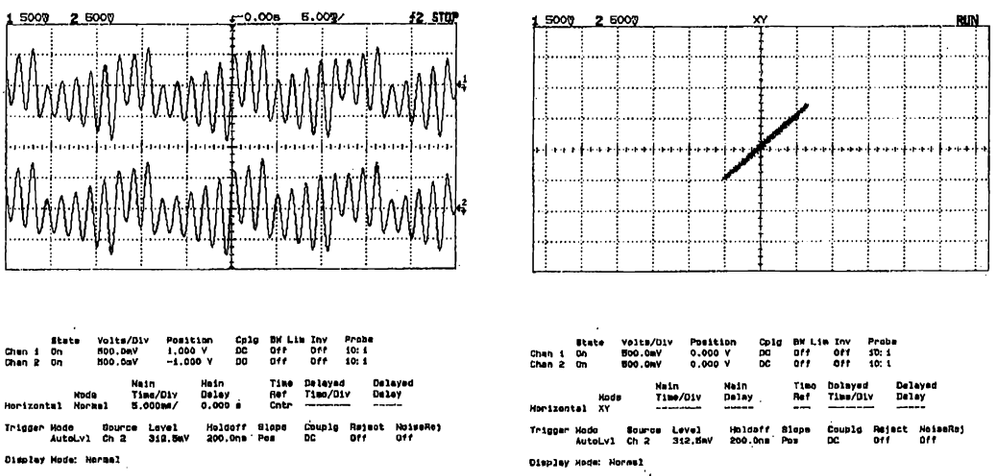

Figure 5.13: Drive and response signals, $V_{C2}(t)$ and $V_{C2}^r(t)$ and V_{C2} *vs* V_{C2}^r

Chapter 6

Conclusion

"The secret to creativity is knowing

how to hide your sources."

Albert Einstein

In this work, we presented a new scheme for the synchronization of chaotic systems by using occasional coupling. We tried first to give historical background then a definition of chaotic motion. Next we selected to present the two most widely studied chaotic systems in literature. Afterwards, we introduced the idea of synchronization of chaotic systems, and stated the different techniques presented in literature. Eventually, we introduced our new scheme of synchronizing chaotic systems.

The aim of our contribution was to exploit the chaotic behavior of several systems to transmit masked information. Our scheme uses the fact that synchronization of some chaotic systems can be reached exponentially fast, and that divergence does not occur instantaneously. Hence, we may switch the response system to an autonomous one, and guarantee that the drive and response systems keep on synchronizing before the error exceeds some predetermined level, beyond which synchronization is considered to be violated, and the systems should be recoupled again via the synchronizing signal.

Although the simulation and experiment results were successful, several improvements on the scheme proposed in this work are possible. The estimates of synchronization and autonomous interval lengths given in chapter four appear to be very conservative. Thus instead of using the Lipschitz constant k, one may use an appropriate Lyapunov exponent associated with the drive system. Moreover, since the divergence of the systems depends on the Lyapunov exponents, one may choose the appropriate system parameters to obtain a chaotic system with a small Lyapunov exponents. This may affect the maximum autonomous phase interval T_a. We expect that as the positive Lyapunov exponents become smaller, T_a gets larger. Hence, an optimum relation between T_s and T_a may also be obtained. The electronic implementation of our system might be improved, in order to transmit useful and meaningful informations.

To the best of our knowledge, our synchronization scheme stands as a novel contribution to the chaotic systems synchronization literature while it displays similarities with methods proposed in [26] and [25]. In fact, the mere practical burden of this method is the presence of high level noise or large parameters mismatch. Nevertheless, the new technology achievement may easily overcome these difficulties. Indeed, laboratory experiments were successful, showing that synchronization had a minimum of robustness, on the other hand, synchronization should not be too robust, because otherwise an intruder could synchronize onto the transmitted signal without precise knowledge of the parameter values. This shows that the design of analog cryptographic systems is still delicate.

At this point of the development, of course, analog cryptography cannot yet compete with the highly developed methods of digital cryptography. However, due to the intense efforts made by researchers in the domain of chaotic synchronization, results are in progress, moreover they are quite promising.

Appendix A

Stability in the Sense of Lyapunov

The following theorems will be stated without a proof. Proofs are available in [32].

Theorem A.1 *The equilibrium point* $\mathbf{0}$ *of the system defined by*

$$\dot{\mathbf{x}}(t) = \mathbf{f}(t, \mathbf{x}) \quad , \quad t \geq 0 \tag{A.1}$$

is uniformly asymptotically stable if there exists a continuously differentiable decrescent locally positive definite function (l.p.d.f) V *such that* $-\dot{V}$ *is an l.p.d.f.*

Theorem A.2 *The equilibrium point* $\mathbf{0}$ *of (A.1) is globally exponentially stable if there exists constants* $a,\ b,\ c > 0,\quad p \geq 1$ *and a continuously differentiable function* $V : \mathbf{R}_+ \times \mathbf{R}^n \rightarrow \mathbf{R}$ *such that*

$$a\|\mathbf{x}\|^p \leq V(t, \mathbf{x}) \leq b\|\mathbf{x}\|^p \ , \tag{A.2}$$

$$\dot{V}(t, \mathbf{x}) \leq \ -c\|\mathbf{x}\| \quad , \quad \forall t \geq 0 \quad , \quad \forall \mathbf{x} \in \mathbf{R}^n \tag{A.3}$$

Theorem A.3 *The equilibrium point* $\mathbf{0}$ *of the system defined by*

$$\dot{\mathbf{x}}(t) = \mathbf{A}(t)\mathbf{x}(t) \quad , \quad t \geq 0 \tag{A.4}$$

is uniformly asymptotically stable if and only if there exist positive constants $M > 0$ *and* $\alpha > 0$ *such that*

$$\|\Phi(t, t_0)\|_i \leq M e^{-\alpha(t-t_0)} \quad , \quad \forall t \geq t_0 \geq 0 \tag{A.5}$$

Systems satisfying (A.5) are some times referred to as being *exponentially stable*, because, if (A.5) holds, the solutions of (A.4) decay exponentially. The import of Theorem (A.3) is thus to show that exponential stability is equivalent to uniform asymptotic stability over $[0, \infty)$.

Appendix B

Bellman-Gronwall Inequality

Theorem B.1 *Suppose $c \geq 0$, $r(.)$ and $k(.)$ are nonnegative valued continuous functions, and suppose*

$$r(t) \leq c + \int_0^t k(\tau) r(\tau) d\tau, \quad \forall t \in [0,T] \tag{B.1}$$

Then

$$r(t) \leq c \ \exp\left[\int_0^t k(\tau) d\tau\right], \quad \forall t \in [0,T] \tag{B.2}$$

proof: Let $s(t)$ denote the right-hand side of (B.1). Then (B.1) states that

$$r(t) \leq s(t) \ , \quad \forall t \in [0,T] \tag{B.3}$$

$$\dot{s}(t) = k(t) r(t) \leq k(t) s(t) \ , \quad \forall t \in [0,T]$$

$$\dot{s}(t) - k(t) s(t) \leq 0 \ , \quad \forall t \in [0,T]$$

$$[\dot{s}(t) - k(t) s(t)] \exp\left[\int_0^t -k(\tau) d\tau\right] \leq 0 \ , \quad \forall t \in [0,T]$$

$$\frac{d}{dt}\left\{s(t) \exp\left[\int_0^t -k(\tau) d\tau\right]\right\} \leq 0 \ , \quad \forall t \in [0,T]$$

$$s(t) \exp\left[\int_0^t -k(\tau) d\tau\right] \leq s(0) = c \ ,$$

$$s(t) \leq c \ \exp\left[\int_0^t k(\tau) d\tau\right] \tag{B.4}$$

Now, (B.4) and (B.3) together imply (B.2). □

Appendix C

Invariance Argument

The following theorem will be stated without a proof. The proof is available in [41].

Theorem C.1 *Let* $D = \{x \in \mathbf{R}^n | \|x\| < r\}$ *and suppose that* $f(t,x)$ *is locally Lipschitz in* x*, uniformly in* t*, on* $[0,\infty) \times D$*. Let* $V : [0,\infty) \times D \to \mathbf{R}$ *be a continuously differentiable function such that*

$$\alpha_1(\|x\|) \leq V(t,x) \leq \alpha_2(\|x\|) \tag{C.1}$$

$$\dot{V}(t,x) = \frac{\partial V}{\partial t} + \frac{\partial V}{\partial x} f(t,x) \leq -W(x) \leq 0 \tag{C.2}$$

$\forall t \geq 0, \forall x \in D$*, where* $\alpha_1(.)$ *and* $\alpha_2(.)$ *are class* $\mathcal{K}$ *functions defined on* $[0,r)$ *and* $W(x)$ *is continuous on* D*. Then, all solutions of*

$$\dot{x} = f(t,x) \tag{C.3}$$

with $\|x(t_0)\| < \alpha_2^{-1}(\alpha_1(r))$ *are bounded and satisfy*

$$W(x(t)) \to 0 \quad as \quad t \to \infty \tag{C.4}$$

Moreover, if all the assumptions hold globally and $\alpha_1(.)$ *belongs to class* $\mathcal{K}_\infty$ *(i.e.* $\alpha_1(\|x\|) \to \infty$ *as* $\|x\| \to \infty$ *continuously in* x*), the statement is true for all* $x(t_0) \in \mathbf{R}^n$*.*

Appendix D

HP-IB Program

This is an HP-IB input deck used to collect data produced by the laboratory experiments of the circuit shown in Figure 5.8.

```
 program measurement;

uses CRT;

{$I c:\tp\hpib\tbpgpib.inc}

const
  multi=1;
  dcsupply=10;
  comp=21;
  scope=5;
var
  ioport,setting : integer;
  i : integer;
  outstr,instr,temp : lstring;
  t : real;
  outfile : text;
```

```
begin
  clrscr;
  assign(outfile,'vvv.dat');
  rewrite(outfile);

  ioport := $2B8;
  setting := 0;
  ieinit(ioport,comp,setting);
  ieabort;
  outstr := 'VSET 2,10';
  ieoutput(dcsupply,outstr);
  delay(200);
  outstr := 'VSET 1,10';
  ieoutput(dcsupply,outstr);
  delay(200);
  t:=0;
(*  ietrig(scope);*)
  delay(1000);
  while (t<50e-3) do
   begin
    outstr := ':MEASURE:SOURCE CHANNEL2';
    ieoutput (scope,outstr);
    delay(500);
    str(t,temp);
    outstr := ':MEASURE:VTIME? '+temp;
    ieoutput(scope,outstr);
    delay(500);
    (*ietrig(scope);*)
    instr := '                ';
    ieenter(scope,instr);
    write(temp,' ',instr);
    write(outfile,temp,'  ');
    write(outfile,instr);
```

```
    outstr := ':MEASURE:SOURCE CHANNEL1';
    ieoutput (scope,outstr);
    delay(500);
    outstr := ':MEASURE:VTIME? '+temp;
    ieoutput(scope,outstr);
    delay(500);
    (*ietrig(scope);*)
    instr := '                ';
    ieenter(scope,instr);
    writeln('  ',instr);
    writeln(outfile,'  ',instr);
    t:=t+0.02e-3;
  end;

  close(outfile);

{  for i:=1 to 100 do
    begin
      str(i/100:4,temp);
      outstr := 'VSET 1,'+temp;
      ieoutput(dcsupply,outstr);

      instr := '            ';
      ieenter(multi,instr);
      writeln(instr);
    end;}

end.
```

References

[1] D. Kaplan and L. Glass. *Understanding Nonlinear Dynamics.* Springer-Verlag, New York, 1995.

[2] E. Atlee Jackson. *Perspectives of Nonlinear Dynamics.* Cambridge University Press, Cambridge, 1990.

[3] F. C. Moon. *Chaotic Vibrations.* John Wiley & Sons, U.S.A, 1987.

[4] S. H. Strogatz. *Nonlinear Dynamics and Chaos.* Addison-Wesley, Massachusetts, 1994.

[5] K. M. Cuomo, A. V. Oppenheim, and S. H. Strogatz "Synchronization of Lorenzed-Based Chaotic Circuits with Applications to Communications," *IEEE Transactions on Circuits and Systems-II*, vol. 40, pp. 626–633, Oct. 1993.

[6] M.P. Kennedy "Three Steps to Chaos- Part II: A Chua's Circuit Primer," *IEEE Transactions on Circuits and Systems-I*, vol. 40, pp. 657–674, Oct. 1993.

[7] L. O. Chua, C. W. Wu, A. Huang, and G. Q. Zhong "A Universal Circuit for Studying and Generating Chaos - Part I : Routes to Chaos," *IEEE Transactions on Circuits and Systems-I*, vol. 40, pp. 732–744, Oct. 1993.

[8] T. Matsumuto, M. Komuro, H. Kokuba, and R. Tokunaga. *Bifurcations: Sights Sounds and Mathematics.* Springer-Verlag, Tokyo, 1993.

[9] Ö. Morgül "Wien bridge based RC chaos generator," *Electronic Letter*, vol. 31, pp. 2058–2059, Nov. 1995.

[10] A. Rodríguez-Vázquez and M. Delgado-Restituto "CMOS Design of Chaotic Oscillators Using State Variables: A Monolithic Chua's Circuit," *IEEE Transactions on Circuits and Systems-II*, vol. 40, pp. 596–613, Oct. 1993.

[11] J. M. Cruz and L. O. Chua "An IC Chip of Chua's Circuit," *IEEE Transactions on Circuits and Systems-II*, vol. 40, pp. 614–625, Oct. 1993.

[12] M. Ogorzalek "Taming Chaos- part I: Synchronization," *IEEE Transactions on Circuits and Systems-I*, vol. 40, pp. 693–699, Oct. 1993.

[13] B. Baird, M. W. Hirsch, and F. Eeckman "A Neural Network Associative Memory for Hand-written Character Recognition Using Multiple Chua Characters," *IEEE Transactions on Circuits and Systems-II*, vol. 40, pp. 667–674, Oct. 1993.

[14] U. Parlitz and L. Kocarev "Multichannel Communication Using Autosynchronization," *Int. J. Bifurcation Chaos*, vol. 6, pp. 581–588, Mar. 1996.

[15] U. Kocarev, L.and Parlitz "General Approach for Chaotic Synchronization with Applications to Communication," *Physical Review Letters*, vol. 74, pp. 5028–5031, Mar. 1995.

[16] C. W. Wu and L. O. Chua "A Simple Way to Synchronize Chaotic Systems with Applications to Secure Communication Systems," *Int. J. Bifurcation Chaos*, vol. 3, pp. 1619–1627, Jun. 1993.

[17] C. W. Wu and L. O. Chua "A Unified Framework for Synchronization and Control of Dynamical systems," *Int. J. Bifurcation Chaos*, vol. 4, pp. 979–998, Apr. 1994.

[18] K. M. Cuomo and A. V. Oppenheim "Circuit Implementation of Synchronized Chaos with Applications to Communications," *Physical Review Letters*, vol. 71, pp. 65–68, Jul. 1993.

[19] A. V. Oppenheim, G. W. Wornell, S. H. Isabelle, and K. M. Cuomo "Signal Processing in the Context of Chaotic Signals," in *PROC. IEEE Int. Conf. Acoustics, Speech and Signal Processing (ICASSP)*, volume IV, pp. 117–120, 1992.

[20] M. Hasler "Synchronization Principles and Applications," in *PROC. ISCAS Tutorial*, chapter 6.2, pp. 314–327. 1994.

[21] U. Feldmann, M. Hasler, and W. Schwarz "Communication by Chaotic Signals: the Inverse System Approach," in *Proc. ISCAS*, 1995.

[22] H. Dedieu, M. P. Kennedy, and M. Hasler "Chaos Shift Keying: Modulation and Demodulation of a Chaotic Carrier Using Self-Synchronizing Chua's Circuit," *IEEE Transactions on Circuits and Systems-II*, vol. 40, pp. 634–642, Oct. 1993.

[23] L. M. Pecora and T. L. Carroll "Synchronization in Chaotic Systems," *Physical Review Letters*, vol. 64, pp. 821–824, Feb. 1990.

[24] L. M. Carroll, T. L.and Pecora "Synchronizing Chaotic Circuits," *IEEE Transactions on Circuits and Systems*, vol. 38, pp. 453–456, Apr. 1991.

[25] L. M. Pecora and T. L. Carroll "Driving Systems with Chaotic Signals," *Physical Review A*, vol. 44, pp. 2374–2383, Aug. 1991.

[26] R. E. Amritkar and N. Gupte "Synchronization of Chaotic Orbits: The Effect of a Finite Time Step," *Physical Review E*, vol. 47, pp. 3889–3895, Jun. 1993.

[27] J. K. John and A. E. Amritkar "Synchronization by Feedback and Adaptive Control," *Int. J. Bifurcation Chaos*, vol. 4, pp. 1687–1695, Jun. 1994.

[28] M. P. Kennedy "Bifurcation and Chaos," in W. K. Chen, ed., *The Circuits and Filters Handbook*, chapter VII-38, pp. 1089–1163. IEEE PRESS, U.S.A, 1995.

[29] K. Murali, M. Lakshmanan, and L. O. Chua "Controlling and Synchronization of Chaos in the Simplest Dissipative Non-Autonomous Circuit," *Int. J. Bifurcation Chaos*, vol. 5, pp. 563–571, Feb. 1995.

[30] K. Murali and M. Lakshmanan "Synchronizing Chaos in Driven Chua's Circuit," *Int. J. Bifurcation Chaos*, vol. 3, pp. 1057–1067, Apr. 1993.

[31] T. L. Carrol and L. M. Pecora "Synchronizing Nonautonomous Chaotic Circuits," *IEEE Transactions on Circuits and Systems-II*, vol. 40, pp. 646–650, Oct. 1993.

[32] M. Vidyasagar. *Nonlinear Systems Analysis.* Prentice-Hall, Englewood Cliffs, 2nd edition, 1993.

[33] Ercan Solak. "Nonlinear Observer Design with Application to the Synchronization of Chaotic Systems,". Master's thesis, Bilkent University, Ankara Turkey, August 1996.

[34] Mario Di Bernardo "An Adaptive Approach to the Control and Synchronization of Continuous-Time Chaotic Systems," *Int. J. Bifurcation Chaos*, vol. 6, pp. 557–568, Mar. 1996.

[35] C. W. Wu, T. Yang, and L. O. Chua "On Adaptive Synchronization and Control of Nonlinear Dynamical Systems," *Int. J. Bifurcation Chaos*, vol. 6, pp. 455–471, Mar. 1996.

[36] Ö. Morgül and E. Solak "On the Observer Based Synchronization of Chaotic Systems," *Physical Review A*, vol. 54, pp. 4803–4811, 1996.

[37] Ö. Morgül and E. Solak. "On the Synchronization of Chaotic Systems by Using State Observers,". To appear in Int. J. Bifurcation Chaos, 1997.

[38] A. Oksasoglu and T. Akgul. "An Indirect Chaotic Signal Masking Approach,". To Appear in IEEE Transactions.

[39] A. Oksasoglu and T. Akgul "A Chaotic Masking Scheme with a Linear Inverse System," *Physical Review Letters*, vol. 75, pp. 4595–4597, Dec. 1995.

[40] Ö. Morgül and M. Feki "On the Synchronization of Chaotic Systems by Using Occasional Coupling," *Physical Review E*, vol. 55, pp. 5004–5009, May 1997.

[41] H. K. Khalil. *Nonlinear Systems.* Macmillan, New York, 1992.

[42] W. Hahn. *Stability of Motion.* Springer-Verlag, New York, 1967.

[43] Ö. Morgül and M. Feki "A Communication Scheme by Using Synchronized Chaotic Systems," in *PROC. IEEE Int. Conf. on Electronics, Circuits, and Systems (ICECS)*, volume II, pp. 1060–1063, 1996.